Estimating the Source of Floating Pumice Found near Torishima Island, Japan: A Back-Tracking Drift Simulation Approach

Tatsu Kuwatani[1], Haruka Nishikawa[1], Yuusuke Tanaka[1], Hiromi Watanabe[2], Noriko Tada[1], Atsushi Nakao[3], Yoshihiko Tamura[4], and Shigeaki Ono[5]

[1]Japan Agency for Marine-Earth Science and Technology
[2]Marine Biodiversity Research Program, Japan Agency for Marine-Earth Science and Technology (JAMSTEC)
[3]Akita University
[4]Kaiyo Kenkyu Kaihatsu Kiko
[5]Kaiyo Kenkyu Kaihatsu Kiko Yokohama Kenkyujo

September 27, 2024

Abstract

Monitoring and detecting marine volcanic activities are key for scientific understanding and disaster prevention. However, this is difficult because they are hidden under water. Near Torishima Island in the Izu Islands, Japan, intensified seismic activity was observed during October 2023, including a mysterious tsunami-triggering earthquake on October 8 (UTC), which was considered to be linked to a volcanic activity. On October 20, 2023, aerial surveys confirmed an 80-km stretch of floating pumice near Torishima Island. This study conducted a Lagrangian back-tracking drift simulation using the ocean current data and surface wind data to trace the origin of the pumice while clarifying the theoretical basis of Lagrangian back-tracking from the Bayesian perspective. Results indicate that the pumice drifted southward from around extensional back-arc basins near Myojinsho Reef and Sumisujima Island approximately 3–5 days before its discovery. These findings are consistent with independent observations such as biological traces and the geochemical characteristics of sampled floating pumice, which is considered identical to that found on October 20 by an airplane. This indicates the presence of unknown volcanic activity around back-arc basins west of the major active volcanic zone. This study demonstrates the utility of combining drift simulations with geochemical and biological data to identify the sources of marine volcanic events, particularly in regions where direct observations are limited. The results of this study contribute to our understanding of volcanic mechanisms and their potential hazards.

Hosted file

`forward_windy00_30days.gif` available at https://authorea.com/users/786281/articles/1226580-estimating-the-source-of-floating-pumice-found-near-torishima-island-japan-a-back-tracking-drift-simulation-approach

Hosted file

`backward_windy00_30days.gif` available at https://authorea.com/users/786281/articles/1226580-estimating-the-source-of-floating-pumice-found-near-torishima-island-japan-a-back-tracking-drift-simulation-approach

Hosted file

`forward_windy10_30days.gif` available at https://authorea.com/users/786281/articles/1226580-estimating-the-source-of-floating-pumice-found-near-torishima-island-japan-a-back-tracking-drift-simulation-approach

Hosted file

backward_windy10_30days.gif available at https://authorea.com/users/786281/articles/1226580-estimating-the-source-of-floating-pumice-found-near-torishima-island-japan-a-back-tracking-drift-simulation-approach

Hosted file

forward_windy50_30days.gif available at https://authorea.com/users/786281/articles/1226580-estimating-the-source-of-floating-pumice-found-near-torishima-island-japan-a-back-tracking-drift-simulation-approach

Hosted file

forward_windy30_30days.gif available at https://authorea.com/users/786281/articles/1226580-estimating-the-source-of-floating-pumice-found-near-torishima-island-japan-a-back-tracking-drift-simulation-approach

Hosted file

backward_windy30_30days.gif available at https://authorea.com/users/786281/articles/1226580-estimating-the-source-of-floating-pumice-found-near-torishima-island-japan-a-back-tracking-drift-simulation-approach

Hosted file

backward_windy50_30days.gif available at https://authorea.com/users/786281/articles/1226580-estimating-the-source-of-floating-pumice-found-near-torishima-island-japan-a-back-tracking-drift-simulation-approach

Estimating the Source of Floating Pumice Found near Torishima Island, Japan: A Back-Tracking Drift Simulation Approach

T. Kuwatani[1], H. Nishikawa[2], Y. Tanaka[2,3], H. K. Watanabe[4], N. Tada[1], A. Nakao[5,1], Y. Tamura[1], and S. Ono[1]

[1]Volcanoes and Earth's Interior Research Center (VERC), Research Institute for Marine Geodynamics (IMG), Japan Agency for Marine-Earth Science and Technology (JAMSTEC), 2-15 Natsushima-cho, Yokosuka, Kanagawa237-0061, Japan .
[2]Research Institute for Value-Added-Information Generation(VAiG), Japan Agency for Marine-Earth Science and Technology, 3173-25 Showa-machi, Kanazawa-ku, Yokohama, Kanagawa 236-0001, Japan
[3]Ocean Eyes Co., Ltd., Uradeyamacho 308, Nakagyo-ku, Kyoto-shi, Kyoto 604-8155, Japan
[4]Institute for Extra-Cutting-Edge Science and Technology Avant-Garde Research (X-Star), Japan Agency for Marine-Earth Science and Technology, 2-15 Natsushima-cho, Yokosuka, Kanagawa237-0061, Japan
[5]Graduate School of Engineering Science, Akita University, Akita 010-8502, Japan

Key Points:

- A back-tracking drift simulation was conducted for floating pumice discovered on October 20, 2023, near Torishima Island in the Izu Islands
- The pumice drifted southward and originated from around back-arc basins near Myojinsho Reef and Sumisujima Island about 3–5 days before
- Results are consistent with petrology, biology, and geochemistry studies and suggest an unknown pumice source

Corresponding author: Tatsu Kuwatani, `kuwatani@jamstec.go.jp`

Abstract

Monitoring and detecting marine volcanic activities are key for scientific understanding and disaster prevention. However, this is difficult because they are hidden under water. Near Torishima Island in the Izu Islands, Japan, intensified seismic activity was observed during October 2023, including a mysterious tsunami-triggering earthquake on October 8 (UTC), which was considered to be linked to a volcanic activity. On October 20, 2023, aerial surveys confirmed an 80-km stretch of floating pumice near Torishima Island. This study conducted a Lagrangian back-tracking drift simulation using the ocean current data and surface wind data to trace the origin of the pumice while clarifying the theoretical basis of Lagrangian back-tracking from the Bayesian perspective. Results indicate that the pumice drifted southward from around extensional back-arc basins near Myojinsho Reef and Sumisujima Island approximately 3–5 days before its discovery. These findings are consistent with independent observations such as biological traces and the geochemical characteristics of sampled floating pumice, which is considered identical to that found on October 20 by an airplane. This indicates the presence of unknown volcanic activity around back-arc basins west of the major active volcanic zone. This study demonstrates the utility of combining drift simulations with geochemical and biological data to identify the sources of marine volcanic events, particularly in regions where direct observations are limited. The results of this study contribute to our understanding of volcanic mechanisms and their potential hazards.

Plain Language Summary

In October 2023, volcanic pumice was found floating over a large area of the ocean near Torishima Island, part of the Izu Island chain, Japan. This occurred during a period of increased seismic activity near Torishima Island, including an earthquake that caused a tsunami, with no clear explanation of its mechanism. We conducted a computer simulation using ocean current data to trace the journey of this pumice backward in time to determine its source. The results of this study suggest that the pumice originated from an unknown underwater volcanic eruption that occurred 3–5 days before the discovery of the floating pumice. The eruption likely occurred around a underwater basin region, which is an area where the Earth's crust is being pulled apart, allowing magma to reach the ocean floor. Our research shows the effectiveness of using such simulations to trace the origins of floating pumice and to identify hidden underwater volcanic activities. Such simulations add to our understanding of the complexities of underwater volcanic activities and their potential hazards.

1 Introduction

Understanding marine volcanic activity, including submarine volcanoes and volcanic islands, and elucidating their formation mechanisms, as well as predicting their activity, are important in academic fields and for disaster prevention and mitigation. However, marine volcanoes are commonly located in remote areas and are hidden under water. Hence, directly observing and monitoring such volcanoes even by geophysical observations and remote sensing are difficult. Therefore, it is challenging to determine the location, scale, and duration of marine volcanic activity.

In the ocean near Torishima Island in the Izu Island chain (Figure 1), seismic activity intensified after October 2, 2023. According to observations by the Japan Meteorological Agency (JMA), four earthquakes with a magnitude (M) of 6.0 or higher were recorded up to October 9. Furthermore, numerous earthquakes occurred after 4:00 A.M. on October 9, including small earthquakes with undetermined epicenters (Japan Meteorological Agency, 2023a). Despite the magnitude of these earthquakes being smaller than those typically expected to generate tsunamis, tsunamis were observed along the Pacific coasts of the Izu–Bonin Islands, Chiba Prefecture, Shikoku, and Kyushu Islands. The mechanisms and causes of these seismic activities and tsunamis, which are potentially related to volcanic activities, are not well understood. Various investigations, including seismological observations, physical exploration, and marine surveys using research vessels, are currently underway to elucidate the details and mechanism of these geological events and to monitor the evolving situation. Additionally, numerous rapid reports were released by organizations such as the National Institute of Advanced Industrial Science and Technology (AIST), Earthquake Research Institute (ERI) at the University of Tokyo, Japan Agency for Marine-Earth Science and Technology (JAMSTEC), and JMA (AIST, 2023a, 2023b; ERI, U Tokyo, 2023; JAMSTEC, 2023a, 2023c, 2023d; Japan Meteorological Agency, 2023b). Recent geophysical studies have clarified the details of earthquakes, revealing that they occurred around Sofu seamount caldera located 20–30 km west of the Sofugan Rock (Fig. 1(b)) (Mizutani & Melgar, 2023; Sandanbata et al., 2024; Kubota et al., 2024; Fujiwara et al., 2024).

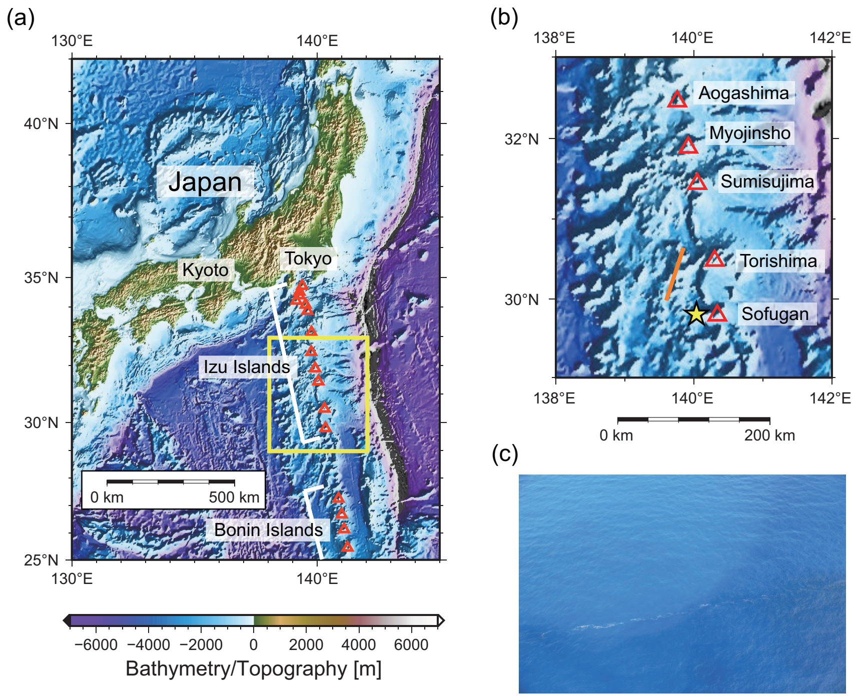

Figure 1. Bathymetric maps of the study area. (a) Japan and the northern part of the Izu–Bonin arc. Red triangles represent active volcanoes in the Izu–Bonin arc, listed by the JMA. (b) Enlarged map of the southern Izu Islands (within yellow framework shown in [a]). Orange line indicates the distribution of the floating pumice observed by the Japan Coast Guard's observation airplane on October 20, 2023 (Japan Coast Guard, 2023b). The location of Sofu seamount is indicated by yellow star. The bathymetric map is based on ETOPO1 (Amante & Eakins, 2009). (c) Floating objects observed by the Japan Coast Guard's observation airplane (shot at 14:25 (JST) October 20, 2023) (Japan Coast Guard, 2023b).

On October 20, 2023, a Japan Coast Guard observation airplane confirmed the presence of pumice floating in the sea scattered over approximately 80 km in a north–south direction about 50 km west of Torishima Island (from 30°41'N, 139°51'E to 29°59'N, 139°36'E) (Japan Coast Guard, 2023b) (Fig. 1). Maritime warnings were issued, and vessels in the vicinity were alerted. An expert noted that there were no recognized active volcanoes in this area, suggesting the possibility of new volcanic activity and, potentially, the formation of a submarine volcanic body. Subsequently, the JMA's research vessel "KEI-FUMARU" collected pumice samples (Japan Meteorological Agency, 2023b), and preliminary petrological descriptions and geochemical analyses were reported (AIST, 2023a, 2023b; ERI, U Tokyo, 2023). These reports suggested that one type of pumice samples may be a part of the same pumice raft. This will be discussed in detail in the Discussion section. However, pumice rafts were not detected in the satellite imagery in the nearby area during this period, and we could not find any evidence in publicly available satellite imagery data including Sentinel.

Drift pumice is often found washed up on coasts. According to Bryan et al. (2004), massive drifts of pumice occur globally every few to several decades. In recent years, significant pumice raft drifting events have occurred, including the 2012 eruption of the Havre Volcano in the Tonga–Kermadec Arc (Jutzeler et al., 2014), the 2019 eruption of the Tonga F Volcano (Jutzeler et al., 2020), and the 2021 eruption of the Fukutoku-Oka-no-Ba submarine volcano (e.g. Tada et al., 2021; Yoshida et al., 2022; Maeno et al., 2022; Fauria et al., 2023). These pumice rafts pose hazards to maritime traffic, fisheries, tourism, and local ecosystems (Jutzeler et al., 2014, 2020). They also serve as crucial physical evidence for understanding the eruption mechanisms of submarine volcanoes, and various studies have been conducted on the formation, floating, and sinking mechanisms and drifting phenomena of pumice produced by submarine volcanic eruptions (e.g. Fauria et al., 2017; Kano, 2003; Cas & Simmons, 2018; Mitchell et al., 2021; Yoshida et al., 2022; Knafelc et al., 2022).

Forward drift simulations, in which a large number of virtual particles are moved in accordance with the flow fields of ocean currents, are effective for predicting the spatial dispersal of pumice. Previous research using drift simulations for predicting the distribution of pumice rafts focused on a previously unknown volcano (0403-91) (Bryan et al., 2004) and Home Reef volcano eruptions (Bryan et al., 2012) along the Tonga arc, the 2012 Havre Volcano eruptions (Jutzeler et al., 2014), and the 2019 Tonga F Volcano eruptions (Jutzeler et al., 2020). Several drift simulations focusing on the pumice drift caused by the 2021 eruption of the Fukutoku-Oka-no-Ba submarine volcano were conducted (Chang et al., 2023; Iskandar et al., 2023; Miyama, 2023). In addition to these studies that simulated actual drift events, forward drift calculations have been conducted for hazard and risk preassessment purposes, assuming eruptions of various submarine volcanoes near Japan (Nishikawa et al., 2023; Kuwatani et al., 2023). Moreover, using simulation results, a preliminary report about the future drift of pumice discovered near Torishima Island was submitted to agencies responsible for volcanic disaster prevention (JAMSTEC, 2023b).

Drift simulations can be used not only for predictions but also for back-tracking estimations (e.g. Van Sebille et al., 2018; Kuroda, 2023). In particular, several research groups conducted back-tracking simulations to estimate the crash location of Malaysia Airlines Flight MH370, which went missing in flight in 2014, based on debris found around the Indian Ocean from 2015 to 2016 (Jansen et al., 2016; Trinanes et al., 2016; Al-Qattan et al., 2023). In addition, our group conducted a back-tracking simulation to estimate the drift start time and path of an ocean bottom electromagnetometer that had been installed on the seafloor of the Nishinoshima Volcano in the Ogasawara Islands and went missing in 2019 (Tada et al., 2021). It was found on the coast of Iriomote Island in the Ryukyu Islands, more than 1,700 km away from the Ogasawara Islands, in February 2021. This research enabled the immediate provision of information to relevant organizations following the eruption of the Fukutoku-Oka-no-Ba submarine volcano in 2021, as we had been studying pumice drifting from the Ogasawara Islands to the Ryukyu Islands and its potential hazards. In addition, Tada et al. (2021) preliminarily mentioned the possibility of exploring unknown submarine volcanoes as a source of pumice, as was conducted in the current study.

This study had two primary objectives: to provide independent insights that contribute to understanding the series of enigmatic geological events occurred near Torishima Island in 2023 and to evaluate the utility of drift simulations in understanding and monitoring submarine volcanic activities. To achieve these objectives, a back-tracking drift simulation using the ocean current data was conducted to estimate the source of the floating pumice discovered near Torishima Island on October 20, 2023, while clarifying the theoretical basis of the back-tracking simulation. The results are compared with other studies that have employed independent approaches (i.e., biological traces and geochemical studies). The connection of the floating pumice to the seismic activity near Torishima Island since October, including the tsunami event occurred on October 9, is also explored. The discussion further includes methodological observations on Lagrangian back-tracking simulations, submarine volcanic activity, and directions for the future research.

2 Back-Tracking Simulation Using Ocean Re-analysis Data

In this section, we initially present a simple theoretical foundation for back-tracking numerical experiments, which have been empirically applied in many studies, using the framework of the Bayesian inversion analysis. We then describe the problem settings and parameters assumed for the drift simulation of the 2023 Torishima floating pumice and present the simulation results.

2.1 Method

Lagrangian data analyses or particle tracking simulations are often used for analyzing floating or suspended organisms and particles in the ocean (e.g. Van Sebille et al., 2018; Kuroda, 2023). The random-walk motion of a Lagrangian particle in a velocity field can be simply expressed using the advection and diffusion terms as follows:

$$\boldsymbol{x}_{t+|\Delta t|} = \boldsymbol{x}_t + \boldsymbol{u}(\boldsymbol{x}_t, t) \cdot |\Delta t| + \sqrt{2D \cdot |\Delta t|} \cdot \boldsymbol{\xi}_{\mathcal{N}}, \tag{1}$$

where $\boldsymbol{x}_t$ is the particle position at time step t; $\boldsymbol{u}(\boldsymbol{x}, t)$ is the velocity field vector at position $\boldsymbol{x}$ and time t; $|\Delta t|$ is a small interval of the time step; D is the diffusion coefficient of the random walk; and $\boldsymbol{\xi}_{\mathcal{N}}$ is a random-number vector in which each element indicates the standard normal distribution. The last term of the right-hand equation represents diffusion due to the random-walk motion, where the standard deviation σ equals $\sqrt{2D \cdot |\Delta t|}$. Because the diffusion process is irreversible, Eq. (1) holds only in the forward time direction. To clearly distinguish between the forward and backward times directions, the absolute value $|\Delta t|$ is used to represent the time step. Equation (1) provides a general and simple formulation for representing the Lagrangian particle motion and is widely used in various natural science fields, including ocean modeling.

Because Eq. (1) represents an irreversible diffusion process, it cannot be directly used for the back-tracking simulation by reversing the sign of either the velocity field $\boldsymbol{u}$ or Δt. In this study, using the Bayesian framework, we try to estimate the past position of the particle from the present position. Bayesian estimation is based on the posterior probability, which is the probability of unknown estimates for a given observable or known values. Using Bayes' theorem, the posterior probability of the one-step-back past position $\boldsymbol{x}_{t-|\Delta t|}$ that yields the present position $\boldsymbol{x}_t$ can be written as follows:

$$p\left(\boldsymbol{x}_{t-|\Delta t|} \mid \boldsymbol{x}_t\right) \propto p\left(\boldsymbol{x}_t \mid \boldsymbol{x}_{t-|\Delta t|}\right) \cdot p\left(\boldsymbol{x}_{t-|\Delta t|}\right), \tag{2}$$

where $p\left(\boldsymbol{x}_t \mid \boldsymbol{x}_{t-|\Delta t|}\right)$ is a likelihood function that can be represented by a general type of probabilistic physical models in the forward time direction and $p\left(\boldsymbol{x}_{t-|\Delta t|}\right)$ is a prior probability using which our prior knowledge regarding the past position can be incorporated into the analysis.

The Lagrangian particle motion equation (Eq. 1) can be directly used as the likelihood function by only shifting one time step backward as $t \to t - |\Delta t|$. Specifically, the likelihood function indicates that $\boldsymbol{x}_t$ shows the Gaussian distribution with a mean of $\bar{\boldsymbol{x}}_t = \boldsymbol{x}_{t-|\Delta t|} + \boldsymbol{u}(\boldsymbol{x}_{t-|\Delta t|}, t)\Delta t$ and variance of $\sigma^2 = 2D \cdot |\Delta t|$. Furthermore, we assume that the prior probability $p\left(\boldsymbol{x}_{t-|\Delta t|}\right)$ has a continuous uniform distribution, in which case there is no useful prior knowledge about the past.

By substituting these expressions into the likelihood function $p\left(\boldsymbol{x}_t \mid \boldsymbol{x}_{t-|\Delta t|}\right)$ and prior probability $p\left(\boldsymbol{x}_{t-|\Delta t|}\right)$ in Eq. (2), the posterior distribution of the previous step is given by

$$p\left(\boldsymbol{x}_{t-|\Delta t|} \mid \boldsymbol{x}_t\right) \propto \exp\left(-\frac{||\boldsymbol{x}_{t-|\Delta t|} - (\boldsymbol{x}_t - \boldsymbol{u}(\boldsymbol{x}_{t-|\Delta t|}, t) \cdot |\Delta t|)||^2}{4D \cdot |\Delta t|}\right). \tag{3}$$

Using this equation, we can probabilistically estimate the previous position $\boldsymbol{x}_{t-|\Delta t|}$ from the present position $\boldsymbol{x}_t$ as a normal distribution with a mean of $\boldsymbol{x}_t - \boldsymbol{u}(\boldsymbol{x}_{t-|\Delta t|}, t) \cdot |\Delta t|$ and variance of $\sigma^2 = 2D \cdot |\Delta t|$. Similar to considering the Lagrangian particle motion equation (Eq. 1) as a probability when substituted to the likelihood function, the posterior probability (Eq. 3) can be directly reversed to a virtual Lagrangian particle motion equation as follows:

$$\boldsymbol{x}_{t-|\Delta t|} = \boldsymbol{x}_t + \boldsymbol{u}_{\mathrm{rev}}(\boldsymbol{x}_t, t) \cdot |\Delta t| + \sqrt{2D \cdot |\Delta t|} \cdot \boldsymbol{\xi}_{\mathcal{N}}, \tag{4}$$

where $\boldsymbol{u}_{\mathrm{rev}}(\boldsymbol{x}_t, t)$ is a reversed velocity field defined as $\boldsymbol{u}_{\mathrm{rev}}(\boldsymbol{x}_t, t) \equiv -\boldsymbol{u}(\boldsymbol{x}_t, t)$. When deriving the above equation, we used the approximation $\boldsymbol{u}(\boldsymbol{x}_{t-|\Delta t|}, t) \sim \boldsymbol{u}(\boldsymbol{x}_t, t)$, which holds in a natural situation where $|\Delta t|$ is sufficiently small and the velocity field does not change abruptly in time and space. Equation (4) is similar to the motion equation that has been empirically used in Lagrangian back-tracking simulations.

2.2 Experimental Settings

Using Eq. (4), we conducted a back-tracking drift simulation of Lagrangian particles to trace back the possible pathways of floating pumices from the region from which they were found (Fig. 1(b)). In this study, the pumice is assumed to horizontally move on the sea surface so that its position $\boldsymbol{x}_t$ indicates a horizontal location, which comprises east–west and north–south coordinates at time t. The horizontal movement of the pumice is known to be driven by a combination of ocean currents, windage, and waves (e.g. Bryan et al., 2004; Jutzeler et al., 2014). Ocean currents and windage are incorporated into the reverse velocity vector field ($\boldsymbol{u}_{\mathrm{rev}}(\boldsymbol{x}, t)$) in the advection term. Furthermore, the effect of waves is included in the diffusion term ($+\sqrt{2D \cdot |\Delta t|} \cdot \boldsymbol{\xi}_{\mathcal{N}}$).

The effect of surface winds on the pumice movement remains a subject of debate in several studies (Jutzeler et al., 2020; Chang et al., 2023; Iskandar et al., 2023; Chiang et al., 2024). In this study, the following four cases are considered for analyzing the effect on the velocity field: no wind effect (0%) and the addition of 1%, 3%, and 5% of the surface wind speed to the velocity field of the ocean current. These windage values are consistent with recent studies: 1–4 % used for the 2019 Tong F pumice (Jutzeler et al., 2020) and 0–2 % (Chang et al., 2023), 2-3% (Iskandar et al., 2023), and 3% (Chiang et al., 2024) for the 2021 Fukutoku-Oka-no-Ba pumice. In addition, our values are consistent with previous simulations for other floating objects, for example, 0 and 1 % employed for a study on pelagic *Sargassum* (Putman et al., 2018) and 0 % for an ocean bottom electromagnetometer (Tada et al., 2021).

The reverse velocity vector field ($\boldsymbol{u}_{\mathrm{rev}}(\boldsymbol{x}, t) \equiv -\boldsymbol{u}(\boldsymbol{x}, t)$) comprises the eastward and northward velocities at position $\boldsymbol{x}$ and time t and is given by the negative of combination of ocean currents and windage (0%, 1%, 3%, and 5% surface wind speed). For ocean currents, we used horizontal velocity obtained from an ocean re-analysis dataset provided for operational numerical weather prediction by Japan Meteorological Agency (2013a). This is daily data, and their horizontal resolution is 0.02° × 0.030303° (2.23 km × 2.89 km) for latitude and longitude, respectively. For surface wind, we used the wave-speed dataset based on the meso-scale model (MSM) reported by JMA (Japan Meteorological Agency, 2024). This is daily data, and their horizontal resolution is $0.05° \times 0.0625°$ (5.57 km $\times$ 5.96 km) for latitude and longitude, respectively. The diffusion term $(+\sqrt{2D \cdot |\Delta t|} \cdot \boldsymbol{\xi}_{\mathcal{N}})$ indicates horizontal diffusion, which comprises east–west and north–south components, each of which is generated by the standard normal distribution. This term is derived from two probabilistic causes: one is a random Brownian motion of particles, called horizontal eddy diffusion, resulting from waves, wind, and other forces in the natural system, and the other is uncertainty. In this study, we set diffusion coefficient D at 10 $\mathrm{m}^2\ \mathrm{s}^{-1}$ based on the general value of horizontal eddy diffusion for small to meso-scale processes (e.g. Okubo, 1971). Note that the equation for particle back-tracking (Equation 4) and the diffusion coefficient are the same as those reported in Tada et al. (2021).

In each experiment, we used 2,600 particles (100 particles at each 26 initial position spaced according to the horizontal resolution of the ocean re-analysis dataset), with the region where the pumice was observed (Fig. 1(b)) being the initial condition. Particles are assumed to move at a depth of 1 m, which corresponds to the shallowest depth in the ocean re-analysis dataset and are released at 00:00 UTC on October 20, 2023. The particles are tracked hourly for 30 days, with the time step $|\Delta t|$ set to 20 min.

2.3 Results

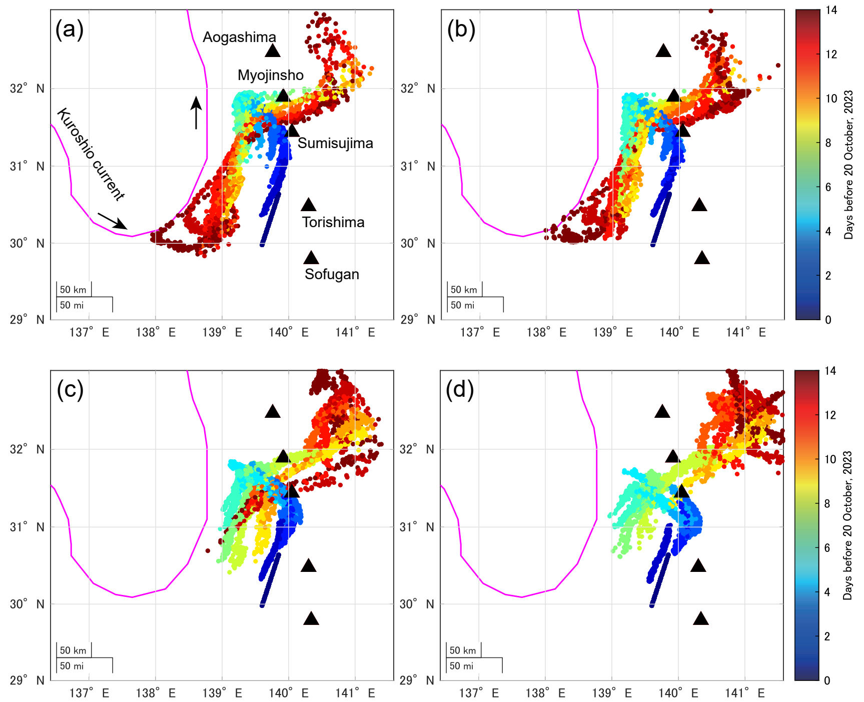

Figure 2. The spatial distribution of particle locations obtained from the back-tracking simulations show each day's distribution. The pseudocolors indicate the number of days the particles were traced back from the start of the drift back-tracking on October 20, 2023 (UTC). Particle locations were traced back for up to 14 days without the effect of wind (a) and with 1% (b), with 3% (c), and (d) 5% effect of wind. Magenta line in each panel represents the Kuroshio Current streamlines during October 10—17, and these data are provided by Japan Coast Guard (2023a).

Figures 2 (a), (b), (c), and (d) show the results of particle tracing back at 0 %, 1%, 3%, and 5% windage, respectively, for up to 14 days. Videos showing the dispersal of the particle distribution over time in the forward and backward time directions for 30 days is available in Supplementary Materials. By comparing the time evolution of the spatial pattern across different cases, they can be classified into two main categories: the weak windage cases (0% and 1%), where windage has no or a negligible effect, and strong windage (3% and 5%), where windage has a significant impact. Below, the temporal change in the spatial pattern is explained for each category. Unless otherwise noted, the explanation will be in the direction of tracing back in time.

For the weak windage (0% (without wind) and 1%) cases (Figure 2(a,b)), in a time-reversed direction, particles initially moved northward, passing west of Sumisujima Island around October 17, and then changed course toward northwest. Around October 14, near the west side of Myojinsho Reef, they started to significantly disperse in the southwest and easterly directions. After the split around October 7, particles that entered the southwest side of Myojinsho Reef were approximately aligned with the Kuroshio Current axis and rode this faster current along its axis, moving up to the vicinity of Kyushu Island within 30 days (refer to Supplementary Materials). Those that moved eastward initially reached the east of the volcanic front and then moved northward near Hachijojima; then, a large portion of the particles rode the Kuroshio Current and moved westward (see the Supplementary Materials).

For 3% and 5% windage cases (Figure 2(c,d)), particles initially moved northward, similar to the weak windage effect cases. They also passed the vicinity area of Sumisujima Island around October 17 and then changed course toward northwest. As the effect of the windage increased, particles tended to take a more easterly path (the front-arc side). Although they moved to the western region of Myojinsho Reef, they were pushed back to a slightly more Southerner area, compared with the weak windage cases. Around October 14, they began to disperse in the southwest and easterly directions. However, they did not split two parts, unlike in the weak windage cases, and most particles moved in the northeast direction and reached the east side of the volcanic front. After drifting in that area for several days, a group of particles rode the Kuroshio Current near Hachijojima and moved westward with the current, similar to the weak windage case. After the ride, particles might escape the Kuroshio Current relatively easily, unlike the weak windage cases (see Supplementary Materials). In fact, a part of particles sometimes moved in the east direction, which might have been caused by the effect of strong windage that might have continued from hours to days, and they came back to the Izu Islands area.

Figure 3 shows the ocean current velocity field on October 15 (UTC). Near N32°, E138°, west of the Myojin Reef, there is a collision point where an east-to-west current collides with the northward-flowing Kuroshio Current. From the southeastern corner of this point, an ocean current flows southward along the west side of the Izu Islands. Particle movements near the discovery date can be interpreted in the forward time direction based on the spatial pattern of the ocean current as follows. In the weak windage cases, two groups of particles emerged: particles that followed the northward Kuroshio Current and those that rode the east-to-west current from the front-arc to the back-arc side. These groups converged near the collision point west of Myojinsho Reef and then moved southward toward the discovery area near Torishima, riding the southward Kuroshio countercurrent. In the strong windage case, all particles moved through the Myojinsho Reef area by riding the east-to-west current and then traveled southward by riding the Kuroshio countercurrent to the discovery area near Torishima .

The overall movement of particles was predominantly governed by stable and consistent ocean currents, which persisted in the same locations over extended periods. In contrast, the wind field, which tends to fluctuate in terms of the direction and speed over short periods, exerted perturbative influences on the particles' movement, particularly during strong windage events. The extent of this impact depended on the intensity of the windage. Differences in the particle behavior between the weak and strong windage cases likely stemmed from the windage effect from the northeast direction. In the strong windage case, the windage likely impeded the inflow of particles from the Kuroshio Current.

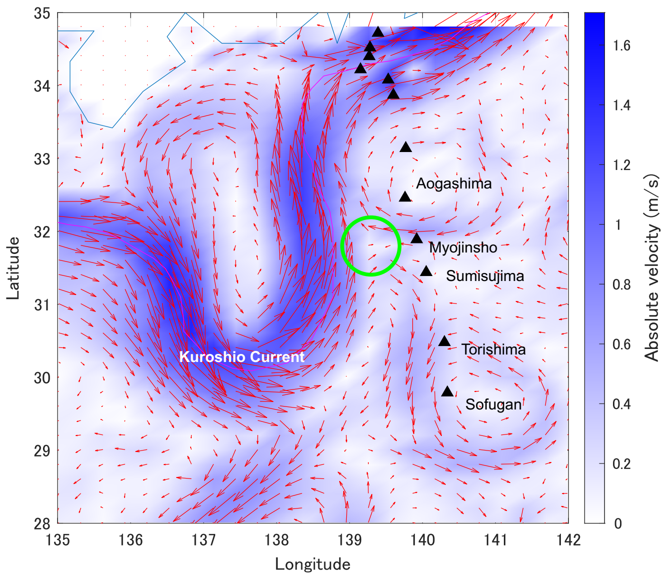

Figure 3. Ocean current patterns on October 15 at 00:00 (UTC). The Kuroshio Current axis is based on the numerical information published by the Japan Coast Guard's Oceanographic Information Division. `https://www1.kaiho.mlit.go.jp/KANKYO/KAIYO/qboc/kurosio-num.html` Green circle indicates a southeastern corner of the collision point where an east-to-west current collides with the northward-flowing Kuroshio Current.

3 Estimating the Spatial and Temporal Source of the Floating Pumice

3.1 Method

By assuming that all pumice particles originated from a single event, we try to estimate the time and location of the pumice origin. This assumption aligned with our intuition that it was unlikely (although not impossible) for pumice widely scattered across the Pacific to have coincidentally gathered. When assuming that the pumice originated from a single event, the following condition is likely to be met: the initial pumice distribution near the source should be concentrated in a narrow region. In other words, we expect to identify a time and location that satisfy this condition to some extent. Here, we evaluate the concentration at a given time t by the spread of distances from the centroid of the point cloud as follows:

$$S(t) = \sqrt{\frac{d_{\mathrm{lon}}^2}{N}\sum_{n=1}^{N}\left(x_{\mathrm{lon},n}(t) - \bar{x}_{\mathrm{lon}}(t)\right)^2 + \frac{d_{\mathrm{lat}}^2}{N}\sum_{n=1}^{N}\left(x_{\mathrm{lat},n}(t) - \bar{x}_{\mathrm{lat}}(t)\right)^2}, \tag{5}$$

where $x_{\mathrm{lon},n}(t)$ and $x_{\mathrm{lat},n}(t)$ are the longitude and latitude of a particle n for time t, respectively; $\bar{x}_{\mathrm{lon}}(t)$ and $\bar{x}_{\mathrm{lat}}(t)$ are the mean values of the longitude and latitude, respectively; N is the total number of particles, and d_{lon} and d_{lat} are the coefficients used to convert differences in the longitude and latitude into distances, respectively. We used 95.42 and 111.32

km for 1° by assuming a latitude of around 31°N. A larger $S(t)$ indicates a lower concentration, whereas a smaller $S(t)$ indicates a higher concentration.

In addition to the pumice concentration, we monitored isotropy as the initial pumice distribution around the source is expected to be isotropic to some extent rather than highly elongated in cases where the pumice raft spans more than several kilometers. For isotropy, we calculated the aspect ratio $\alpha(t)$ from the ratio of the eigenvalues obtained by the eigenvalue decomposition of the covariance matrix of the point cloud coordinates.

$$\alpha(t) = \sqrt{\lambda^{\mathrm{I}}(t)/\lambda^{\mathrm{II}}(t)}, \tag{6}$$

where $\lambda^{\mathrm{I}}(t)$ and $\lambda^{\mathrm{II}}(t)$ represent the larger and smaller eigenvalues at time t, respectively. An aspect ratio closer to 1 indicates isotropy, whereas a ratio closer to 0 indicates a highly elongated, straight-line distribution.

3.2 Results

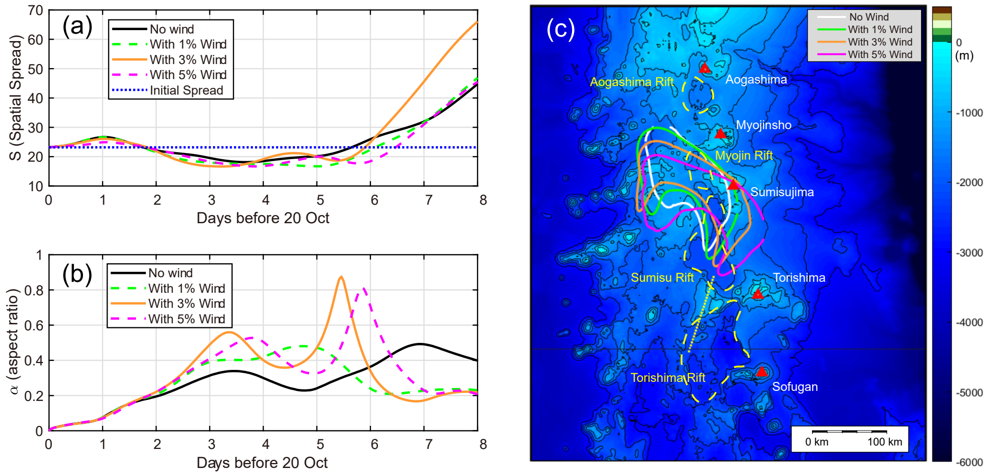

Figure 4. Results of the pumice source estimation. The time evolution of the spatial spread (a) and aspect ratio (b) are shown as time progresses backward from 00:00 on October 20 (UTC), corresponding to the discovery of the floating pumice. In (a), blue dotted line represents the initial spread value, which serves as the criteria for identifying a small spread value. (c) Spatial distribution of pumice particles when the spread is lower than the initial distribution observed on October 20. Using kernel density estimation, a contour line representing the 95% credible region is shown for each case: without wind effect (white) and 1% (green), 3% (orange), and 5% (magenta) wind. In (c), the initial positions of particles and active volcanoes are marked by small yellow circles and red triangles, respectively. The location of the Sofu seamount is indicated by a white star, and back-arc rifts are shown by yellow dashed lines.

Figures 4(a) and (b) show the temporal evolution of the spread $S(t)$ and the aspect ratio $\alpha(t)$, respectively. Regardless of the effect of windage, the spread initially increased slightly and then decreased as time was traced back from the discovery of the floating pumice. It then bottomed out at around 89 h (3 days and 17 hours) for without wind case and at 120 h (5 days) for 1% wind case, 78 h (3 days and 6 hours) for 3%

wind case, and 94 h (3 days and 22 hours) for 5% wind case. Subsequently, all cases exhibited a monotonically increasing trend with a steep slope from around 5–7 days. For all cases, the aspect ratio initially started from zero as it is distributed in a straight line, which is a simplified representation of the pumice observed on October 20, and exhibited the first peak around 3–5 days. It demonstrated distinct second peaks around 5–7 days for the 0%, 3%, and 5% cases, while it did not increase so largely for the 1% windy case.

Because the spread did not show a distinct minimum value in each case, identifying the source timing at the hour or one-day scale was difficult. However, it was considered to be around 3–5 days for all cases based on the time at which the spread exhibited a low value, similar to the minimum value for each case. The spread and aspect ratios showed extreme values (the first peak) at a similar time for each case. The source region was assumed to be the area with a dense particle distribution when the spread $S(t)$ is at its lowest.

Figure 4(c) shows the estimated source region overlaid on the seafloor topography. As mentioned earlier, the spread values did not display distinct minima in any of the cases; instead, they exhibited similar values over several days. To establish uniform and objective criteria while minimizing the risk of missing the source region and avoiding over interpretation, we set the threshold as inclusively as possible: the source timing was defined as the period when the spread values are smaller than the initial observed value and source region corresponded to an area containing 95% of particles. The estimated source regions were generally located on the back-arc side, including the northern part of the Sumisu Rift, Myojin Rift, and Sumisu Caldera. In the stronger windage cases, there was a slight shift toward the fore-arc side and southern regions, in comparison to the weaker windage cases.

4 Discussion

4.1 Lagrangian back-tracking simulation

Note that the Lagrangian back-tracking equation (Eq. 4) cannot either be interpreted as an equation of motion in the real physical world nor can it be physically and mathematically derived from the original forward Lagrangian equation alone properly. However, it can be regarded as an equation of motion for a virtual particle used in the probabilistic estimation of the past position in inversion analysis and can be properly derived through the Bayesian framework. Such a probabilistic particle representation is commonly employed in many inversion problems, such as in the Markov chain Monte Carlo algorithm (e.g. Metropolis et al., 1953; Gilks et al., 1995), and has been widely applied in Earth material sciences (e.g. Kuwatani et al., 2012; Morishige & Kuwatani, 2020; Matsumura et al., 2021).

Furthermore, probabilistic particle expressions for the time evolution of unknown variables are employed in data assimilation through sequential Monte Carlo algorithms, also known as particle filters, (e.g. Kitagawa, 1987; Doucet et al., 2000), and have been applied to Earth material sciences (e.g. Omori et al., 2016; Kuwatani et al., 2018; Ito et al., 2021). In adjoint-based data assimilation, used to estimate past states following an advection-diffusion equation, the diffusion term (with its sign reversed relative to the normal advection term) also appears in an adjoint equation for backward calculations, similar to Eq. (4). Ismail-Zadeh et al. (2004) demonstrated that this inverted diffusion term is necessary to accurately estimate a diffusive physical variable, such as heat, in a past state. Therefore, Eq. (4) can be seen as an approximate representation of the uncertainty in estimating particle positions, which increases as we move backward in time, and manifests as a diffusion term from a macroscopic view.

Although we adopted the Lagrangian particle simulation approach to trace the backward paths of the pumice in this study, we did not exclude the possibility of using other approaches to estimate past particle positions. Recently, we have developed advanced adjoint-based data assimilation methods that integrate Eulerian and Lagrangian perspectives to estimate the past state from the present state of the Earth's interior (Nakao et al., 2024a, 2024b). Further development of these methods may allow for the more precise estimate of particle trajectories compared with using only the Lagrangian method and also provide insights into reconstructing macroscopic velocity fields in which particles move.

4.2 Origin of the Pumice

The results of the back-tracking simulation suggest that the floating pumice drifted southward from the back-arc rift area located west of active volcanic fronts, such as Myojinsho Reef and Sumisujima Island, finally arriving at the position where it was found on October 20. This leads to the natural conclusion that the drifting pumice found near Torishima Island on October 20 via the airplane observation is unlikely to be directly related to a seismic activity near Torishima Island; more specifically, it is not related to Sofu seamount that occurred in October, particularly the earthquake event on October 8 (UTC) that caused an unexplained tsunami, which is considered to be related to a submarine volcanic activity. Instead, it seems likelier that they have different origins.

Because it is unlikely that the pumice originally spread over a wide area and coincidentally gathered, its source is presumed to have appeared after October 15 when particles began to widely disperse in the time-reverse direction under the influence of the Kuroshio Current and east-to-west current (Figure 2). Our analysis of the concentration and aspect ratio of the simulated particle cloud indicates that areas including the Myojin Rift, Sumisu Rift, and Sumisu caldera are reasonable source regions. The area east of the presumed source area, Bayonnaise Rocks including Myojinsho Reef, is located on a volcanic front, which is part of an active caldera, the Myojinsho caldera; additionally, several eruptions have occurred here over the past century, often accompanied by the formation and disappearance of islands (Japan Meteorological Agency, 2013b). In 1953, a research vessel encountered an eruption in this area, leading to a tragic incident in which 31 crew members lost their lives, and a tsunami was also observed. Eruption warnings have been continuously issued around Bayonnaise Rocks (Myojinsho Reef) since January 26, 2023 based on discolored water. Furthermore, Sumisu caldera also generates tsunamis approximately once every ten years caused by subsidence through trapdoor faults (Sandanbata et al., 2022).

In the extensional back-arc basins, called the back-arc rift zone, which is included by the estimated source of the pumice in this study, there is no direct evidence for the presence of active volcanoes. Deep-sea drilling in the Sumisu Rift has shown that the upper layers of sediment predominantly consist of pumice, suggesting submarine calderas or back-arc rifts as primary sources (Fujioka, 1989). Moreover, near the Myojin Knoll, located just east of the back-arc rift (approximately 40 km south of Aogashima and about 25 km north of the Bayonnaise Rocks), diving surveys by "Shinkai 2000" have confirmed that the caldera walls are composed of pumice. These surveys have also identified blocks of pumice larger than 1 m (Yuasa, 1995) on the seafloor.

The observed pumice raft area was roughly estimated to be 0.1–1 km^2 based on its length of about 80 km reported by (Japan Coast Guard, 2023b) and width of about 1–10 m roughly estimated by visualizing the photo Japan Coast Guard (2023b). The estimated area was considerably less than the recent reports of the actually observed area of the pumice raft: 1,600 km^2 for the 2006 Home Reef Volcano in Tonga (Bryan et al., 2012), 400 km^2 for the 2012 Havre eruption (Jutzeler et al., 2014), 195 km^2 for the 2019 Tonga F eruption (Jutzeler et al., 2014), and 290 km^2 for Fukutoku-Oka-no-Ba (Ikegami, 2021). The pumice found near Torishima was likely too minor to be detected via routine satellite observations, and the volcanic activity from which it originated might be of such a low intensity that it was not recognized in distant monitoring systems such as seismic observations.

The small volume of the drifting pumice indicated the possibility of the re-activation of the pumice that had previously washed ashore. The estimated source area included Sumisujima volcanic island (Fig. 4), which might be a potential source region for this re-activation. While our simulation did not exclude this possibility, AIST (2023a) reported that the likelihood of re-activation is low based on the geological observations of the sampled pumice, as discussed later.

4.3 Sampling Floating Pumice

Following the discovery of the pumice near Torishima Island by the observation aircraft, the JMA's oceanographic observation ship "KEIFUMARU," sailed from October 27–31 in the area from 28°N138°E to 30°N140°E to search for the pumice (Japan Meteorological Agency, 2023b). They sampled the pumice scattered on the sea surface southwest of Torishima Island at ca. 100 km from Torishima Island.

White pumice was collected around 12:00 on October 27 (JST) at N29°18′, E140°00′. They mostly have sizes of 1 cm to several centimeters, with the largest being slightly over 10 cm (Japan Meteorological Agency, 2023b). According to AIST (2023a), the preservation of fragile surface structures, predominantly angular shapes, and the almost absence of biological attachments excludes the possibility of them being drifted for a long period of several months or more. For similar reasons, the possibility of them being redrifted beach-deposited pumice is considered low (AIST, 2023a). Therefore, it is considered that the white pumice had been recently produced by volcanic activity, and AIST (2023a) concluded that it is highly likely to be part of the pumice raft observed from the air by the Japan Coast Guard on October 20 (JST).

In addition to white pumice, "KEIFUMARU" collected another pumice type, gray pumice, on October 27, 28, and 31 (JST), at locations N29°54′,E139°34′, N29°54′,E139°32′, and N29°02′,E138°00′, respectively (Japan Meteorological Agency, 2023b; AIST, 2023a). The sampling location of gray pumice was several tens of kilometers far away from that of the white pumice. Most of this pumice is well-rounded, with the largest being approximately 3 cm, and many others being fine-grained, less than 1 cm, as seen in the published photos. The pumice universally has biological remains attached, particularly many serpulid worm tubes, approximately 1 mm in diameter. Serpulid worms are relatively late colonizers (c.a. 6 months) of floating material (Mesaglio et al., 2021). In addition, the pumice found on October 31 was reported to be scattered with plastic waste (Japan Meteorological Agency, 2023b). These characteristics suggest long-term drifting, indicating that the gray pumice had either drifted for an extended period or underwent repeated re-drifting. AIST (2023b) concluded that this pumice was likely sourced from the 2021 eruption of Fukutoku-Okanoba, based the chemical composition of the basaltic glass and the presence of dark inclusions similar to the drifting pumice reported by Yoshida et al. (2022). Clear differences in the sample location, biological attachment, and geochemistry between the white and gray pumices exclude the possibility of their coexistence within the same pumice raft during their drifting.

4.4 Implications of Marine Organisms Attached to White Pumice

According to the AIST's November 7, 2023, report (AIST, 2023a), the white pumice collected by "KEIFUMARU" around 12:00 on October 27 had almost no attached biological remains, with only three goose barnacles less than 4 mm in length attached. Based on their morphological characteristics, they were identified as *Lepas anserifera*.

Lepas barnacles are rapid colonizers of floating materials (< 17 days), and their growth rate in the capitular-length direction ranges from 0.33 to 1.45 mm/day (MacIntyre, 1966; Inatsuchi et al., 2010; Mesaglio et al., 2021; Watanabe et al., 2024) The size of its cyprid or settlement-stage larvae is approximately 1.3 mm; therefore, it is plausible that Lepas barnacles settled on the pumice formed and released less than approximately 20 days before collection.

Although growth rates vary depending on the environment, based on these experimental growth rates, it is unlikely that *L. anserifera* attached more than half a month before collection on October 27. This is consistent with the fact that the pumice is the same as that observed by the aircraft on October 20.

4.5 Implications of Geochemical Characteristics of White Pumice

According to ERI, U Tokyo (2023) and AIST (2023a), the whole-rock chemical composition obtained via XRF analysis indicated dacitic to rhyolitic compositions with the SiO_2 contents ranging from 70.5 to 74.6 wt.% and the $Na_2O + K_2O$ contents ranging from 6.3 to 6.7 wt.%. These compositions differ from the recent eruptive products of active volcanoes on the volcanic front of the Izu–Ogasawara region (e.g., Nishinoshima, Iwo Jima, and Fukutoku-Okanoba). Additionally, ERI, U Tokyo (2023) and AIST (2023a) suggested that these pumices might be derived from rhyolitic volcanoes distributed along the back-arc rift zone west of the volcanic front (e.g., the Torishima depression). Furthermore, the whole-rock trace element composition (i.e., Ba/La and La/Sm) showed values similar to those of volcanic ejecta from submarine volcanoes in the back-arc rift zone (North and South Sumisu Basins, Hachijo Basin), as reported by AIST (2023b).

Tamura et al. (2009) geochemically identified three types of Quaternary rhyolites in the Izu-Ogasawara arc front, which are closely related in terms of the volcano type and crustal structure. The predominantly basaltic islands in the volcanic front produce small volumes of rhyolites (R1), submarine calderas in the volcanic front erupt mostly rhyolites (R2), and seamounts, knolls, and pillow ridges in the back-arc extensional zone are mostly basaltic but also contain rhyolites (R3). In addition to the possibility that the white pumice corresponded to R3 (ERI, U Tokyo, 2023; AIST, 2023b), we proposed that it might correspond to R2.

The back-tracking drift simulation used in this study demonstrated that the floating pumice drifted southward around the back-arc rift on the west side of the active volcanic front, reaching the observation position on October 20. Additionally, the source analysis suggested that the pumice could have originated from around the back-arc side of the Sumisujima and Myojinsho area, which included the back-arc extensional zone as well as submarine caldera or submarine volcanoes. The simulation results were consistent with geochemical analyses.

4.6 Pumice Tracing to Infer Hidden Submarine Volcanism

While some submarine volcanic eruptions, such as the 2021 Fukutoku-Oka-no-Ba and 2022 Hunga Tonga–Hunga Ha'apai eruptions, were clearly observed by geophysical measurements and confirmed visually, others, such as the 2012 Havre and 2019 Tonga F eruptions, were recognized only after the discovery of pumice rafts and subsequent investigations to identify the eruptions. In addition, deep-sea submarine volcanoes are generally believed to exhibit effusive rather than explosive eruptions (Kano, 2003; Allen et al., 2010; Manga et al., 2018; Cas & Simmons, 2018), making it extremely challenging to detect these volcanic activities. AIST (2023a) reported that the white pumice discovered near Torishima Island notably lacked prominent quench textures, indicating that eruption occurred in deep-sea rather than in shallow waters. While detailed satellite imagery investigations have identified eruptions, such as Havre in 2012 and Tonga F in 2019, it is particularly difficult to detect smaller-scale eruptions from satellite images because they produce less pumice and are presumably smaller in scale. At present (September 2024), there have been no reports of such traces being found by satellite imagery for eruptions related to the pumice found on October 20.

However, such "unknown" eruptions of submarine volcanoes that eject small amounts of pumice might usually go undetected and therefore, might be not as rare as thought. This study represents the first case in which a back-tracking drift simulation has proven effective in pinpointing the eruption sites of such unknown submarine volcanoes. In the future, by using satellite imagery observations and autonomous drones, it might be possible to automatically detect pumice rafts (e.g. Zheng et al., 2022). Combining this with back-tracking simulations, numerous small-scale submarine volcanic activities that were previously invisible could be detected. In addition to locating the eruption site, detailed analyses of the pumice microstructures and in situ marine surveys are expected to contribute to elucidating the eruption mechanisms and monitoring of submarine volcanic activities.

5 Conclusion

Our study conducted back-tracking drift simulations of floating pumice found near Torishima Island in the Izu–Ogasawara Islands on October 20, 2023. By integrating the ocean current data and surface wind data, we traced the pumice's journey, revealing its likely origin as near the back-arc side region west of Myojinsho and Sumisujima Island 3–5 days before its discovery. This timing and location are not consistent with either the increased seismic activity observed in the region since October or the unexplained tsunami-accompanied earthquake on October 9.

These findings suggest that the pumice originated from an unknown volcanic event, possibly distinct from the activities of known active volcanic sites in the area. Preliminary reports (AIST, 2023a, 2023b; ERI, U Tokyo, 2023) suggest that geochemical analyses indicated a composition consistent with volcanoes in the back-arc rift zone, and the lack of extensive biological traces on the pumice implies a relatively recent eruptive source (AIST, 2023a). These results highlight the significance of back-tracking drift simulations in uncovering hidden submarine volcanic activities and their potential impacts.

Furthermore, our research underscores the challenges in detecting and understanding deep-sea volcanic activities, especially those that are effusive and not immediately apparent. By combining drift simulations with geological, petrological, and biological analyses, we can gain a more comprehensive understanding of such phenomena. This approach not only aids in identifying the sources of marine volcanic events but also contributes to the broader field of submarine geology and volcanic hazard assessment.

6 Open Research

The ocean re-analysis dataset is the operational system for monitoring and forecasting coastal and open-ocean states around Japan GPV, provided by the Japan Meteorological Business Support Center (`http://www.jmbsc.or.jp/en/index-e.html`). The maps in Figure 1 were produced using Generic Mapping Tools v5 (Wessel et al., 2013).

Acknowledgments

This work was supported by JST CREST (JPMJCR1761)and JSPS KAKENHI (JP 20H01986; 21H04750; 22H00251; JP24K01139); and the Cooperative Research Program of the Earthquake Research Institute, University of Tokyo (ERI JURP 2021-B-01; 2022-B-06). The authors thank Dr. S. Tanaka for his comments on the geophysical observation of volcanic activities. The authors also thank Prof. S.E. Bryan and Prof. M. Jutzeler for their constructive comments on the early version of the manuscript.

References

AIST. (2023a, November 7). *Characteristics of the drifting pumice collected near torishima in october 2023 (first report) (in Japanese).* Report for Coordinating Committee for Prediction of Volcanic Eruption `https://www.gsj.jp/hazards/volcano/kazan-bukai/yochiren/torishimakinkai_231109_1.pdf`. (Retrieved on November 26, 2023)

AIST. (2023b, November 15). *Characteristics of the drifting pumice collected near torishima in october 2023 (second report) (in Japanese).* Report for Coordinating Committee for Prediction of Volcanic Eruption `https://www.gsj.jp/hazards/volcano/kazan-bukai/yochiren/torishimakinkai_231115_1.pdf`. (Retrieved on November 26, 2023)

Allen, S. R., Fiske, R. S., & Tamura, Y. (2010). Effects of water depth on pumice formation in submarine domes at Sumisu, Izu-Bonin arc, western Pacific. *Geology*, *38*(5), 391–394.

Al-Qattan, N., Herbert, G. S., Spero, H. J., McCarthy, S., McGeady, R., Tao, R., & Power, A.-M. (2023). A stable isotope sclerochronology-based forensic method for reconstructing debris drift paths with application to the MH370 crash. *AGU Advances*, *4*(4), e2023AV000915. doi: https://doi.org/10.1029/2023AV000915

Amante, C., & Eakins, B. W. (2009). ETOPO1 arc-minute global relief model: procedures, data sources and analysis. Retrieved from `https://repository.library.noaa.gov/view/noaa/1163`

Bryan, S. E., Cook, A., Evans, J., Colls, P., Wells, M., Lawrence, M., ... Leslie, R. (2004). Pumice rafting and faunal dispersion during 2001–2002 in the Southwest Pacific: record of a dacitic submarine explosive eruption from Tonga. *Earth and Planetary Science Letters*, *227*(1-2), 135–154.

Bryan, S. E., Cook, A. G., Evans, J. P., Hebden, K., Hurrey, L., Colls, P., ... Firn, J. (2012). Rapid, long-distance dispersal by pumice rafting. *PloS one*, *7*(7), e40583.

Cas, R. A. F., & Simmons, J. M. (2018). Why deep-water eruptions are so different from subaerial eruptions. *Frontiers in Earth Science*, *6*. doi: 10.3389/feart.2018.00198

Chang, Y.-L. K., McIntosh, I. M., Miyama, T., & Miyazawa, Y. (2023). Projection of August 2021 pumice dispersion from the Fukutoku-Oka-no-Ba eruption in the western North Pacific. *Scientific Reports*, *13*(1), 3945.

Chiang, Y., Huang, P.-C., & Yang, Z.-Y. (2024). Assessment of the fukutoku-okanoba pumice rafts dispersion model using the daily collection data from nuclear power plants seawater intake system. *Nuclear Engineering and Design*, *427*, 113448.

Doucet, A., Godsill, S., & Andrieu, C. (2000). On sequential monte carlo sampling methods for bayesian filtering. *Statistics and computing*, *10*, 197–208.

ERI, U Tokyo. (2023, November 9). 【*Analysis Results*】 *Whole-rock Chemical Composition of Drifting Pumice Collected Near Izu Torishima and Sofugan Rocks (in Japanese).* Report for Coordinating Committee for Prediction of Volcanic Eruption `https://www.eri.u-tokyo.ac.jp/eq/20272/`. (Retrieved on November 26, 2023)

Fauria, K. E., Jutzeler, M., Mittal, T., Gupta, A. K., Kelly, L. J., Rausch, J., ... Retailleau, L. (2023). Simultaneous creation of a large vapor plume and pumice raft by the 2021 fukutoku-oka-no-ba shallow submarine eruption. *Earth and Planetary Science Letters*, *609*, 118076.

Fauria, K. E., Manga, M., & Wei, Z. (2017). Trapped bubbles keep pumice afloat and gas diffusion makes pumice sink. *Earth and Planetary Science Letters*, *460*, 50–59.

Fujioka, K. (1989). Arc volcanism and rifting. *Nature*, *342*(1), 18–20.

Fujiwara, T., Imai, K., Obayashi, M., Yoshida, K., Tada, N., Obana, K., ... Kodaira, S. (2024). The sofu seamount present in the source area of the october 2023 earthquake and tsunami in japan. *Geophysical Research Letters*.

Gilks, W. R., Richardson, S., & Spiegelhalter, D. (1995). *Markov chain monte carlo in practice.* CRC press.

Ikegami, F. (2021). Pumice raft dispersion of fukutoku-oka-no-ba 2021 eruption. *Abstract Vol. Annu. Meet. Volcanol. Soc. Jpn. 2021*, A2-02.

Inatsuchi, A., Yamato, S., & Yusa, Y. (2010). Effects of temperature and food availability on growth and reproduction in the neustonic pedunculate barnacle lepas anserifera. *Marine Biology*, *157*, 899–905.

Iskandar, M. R., Park, Y.-G., Kim, K., Jin, H., Seo, S., & Kim, Y. H. (2023). Tracking the pumice rafts from the Fukutoku-Okanoba submarine volcano with satellites and a Lagrangian particles trajectory model. *Marine Pollution Bulletin*, *193*, 115254. doi: https://doi.org/10.1016/j.marpolbul.2023.115254

Ismail-Zadeh, A., Schubert, G., Tsepelev, I., & Korotkii, A. (2004). Inverse problem of thermal convection: numerical approach and application to mantle plume restoration. *Physics of the Earth and Planetary Interiors*, *145*(1-4), 99–114.

Ito, M., Kuwatani, T., Oyanagi, R., & Omori, T. (2021). Data-driven analysis of nonlinear heterogeneous reactions through sparse modeling and bayesian statistical approaches. *Entropy*, *23*(7), 824.

JAMSTEC. (2023a, October 30). *About the Seismic Activity Near Torishima in October 2023 and the Tsunami that was Disproportionately Large Compared to the Earthquake Magnitude (in Japanese).* Column by researchers `https://www.jamstec.go.jp/j/pr/topics/column-20231030/`. (Retrieved on November 26, 2023)

JAMSTEC. (2023b, October 24). *Future Drift of the Floating Pumice Observed Near Torishima (Preliminary Rapid Report) (in Japanese).* Report for Coordinating Committee for Prediction of Volcanic Eruption `https://www.jamstec.go.jp/rimg/j/topics/20231026/`. (Retrieved on November 26, 2023)

JAMSTEC. (2023c, November 8). *Regarding an Emergency Survey Voyage in the Waters near Torishima by the Oceanographic Research Ship 'Kaimei' (in Japanese).* Press Release `https://www.jamstec.go.jp/j/about/press_release/20231108/`. Retrieved 2023-11-26, from `https://www.jamstec.go.jp/j/about/press_release/20231108/` (Retrieved on November 26, 2023)

JAMSTEC. (2023d, November 21). *Regarding an Emergency Survey Voyage in the Waters near Torishima by the Oceanographic Research Ship 'Kaimei' (Preliminary report) (in Japanese).* Press Release `https://www.jamstec.go.jp/j/about/press_release/20231121/`. (Retrieved on November 26, 2023)

Jansen, E., Coppini, G., & Pinardi, N. (2016). Drift simulation of MH370 debris using superensemble techniques. *Natural Hazards and Earth System Sciences*, *16*(7), 1623–1628. doi: 10.5194/nhess-16-1623-2016

Japan Coast Guard. (2023a). *Kuroshio current axis. [Data]* [dataset]. Retrieved from `http://www.mirc.jha.jp/products/KCP/`

Japan Coast Guard. (2023b, October 20). *Regarding the floating objects near Torishima observed on October 20th (in Japanese).* `https://www.kaiho.mlit.go.jp/info/kouhou/post-1041.html`. (Retrieved on November 26, 2023)

Japan Meteorological Agency. (2013a). Meso-Scale Model (JMA-MSM1206). Outline of the operational numerical weather prediction at the Japan Meteorological Agency. *JMA*, 71–93. Retrieved from `http://www.jma.go.jp/jma/jma-eng/jma-center/nwp/outline2019-nwp/index.htm`

Japan Meteorological Agency. (2013b). National Catalogue of the Active Volcanoes in Japan, 4th Edition. Retrieved from `https://www.data.jma.go.jp/svd/vois/data/tokyo/STOCK/souran_eng/menu.htm`

Japan Meteorological Agency. (2023a, October 9). *Report on Earthquake near Torishima Island around 5:25 on October 9, 2023 (2nd report) (in Japanese).* `https://www.jma.go.jp/jma/press/2310/09b/202310091100.html`. (Retrieved October 19, 2023)

Japan Meteorological Agency. (2023b, November 1). *Sampling of Pumice in the Waters Near Torishima by the Marine Meteorological Observation Ship 'Keifu-Maru (in Japanese).* Press Release Materials for Fiscal Year 2023 `https://www.jma.go.jp/jma/press/2311/01b/20231101_keihu-karuishi.html`. (Retrieved on November 26, 2023)

Japan Meteorological Agency. (2024). Meso-scale model (MSM) grid data, Information catalog of Japan Meteorological Agency. Retrieved from `https://www.data.jma.go.jp/suishin/cgi-bin/catalogue/make_product_page.cgi?id=MesModel`

Jutzeler, M., Marsh, R., Carey, R. J., White, J. D., Talling, P. J., & Karlstrom, L. (2014). On the fate of pumice rafts formed during the 2012 Havre submarine eruption. *Nature communications*, *5*(1), 3660.

Jutzeler, M., Marsh, R., van Sebille, E., Mittal, T., Carey, R. J., Fauria, K. E., … McPhie, J. (2020). Ongoing dispersal of the 7 August 2019 pumice raft from the Tonga arc in the southwestern Pacific Ocean. *Geophysical Research Letters*, *47*(5), e1701121.

Kano, K. (2003). Subaqueous pumice eruptions and their products: A review. *Washington DC American Geophysical Union Geophysical Monograph Series*, *140*, 213–229.

Kitagawa, G. (1987). Non-gaussian state—space modeling of nonstationary time series. *Journal of the American statistical association*, *82*(400), 1032–1041.

Knafelc, J., Bryan, S. E., Jones, M. W., Gust, D., Mallmann, G., Cathey, H. E., … Howard, D. L. (2022). Havre 2012 pink pumice is evidence of a short-lived, deep-sea, magnetite nanolite-driven explosive eruption. *Communications Earth & Environment*, *3*(1), 19.

Kubota, T., Sandanbata, O., Saito, T., & Matsuzawa, T. (2024). Accelerating seafloor uplift of submarine caldera near sofugan volcano, japan, resolved by distant tsunami recordings. *Geophysical Research Letters*, *51*(12), e2024GL108415.

Kuroda, H. (2023). History, current status, and future vision of particle-tracking simulation applied to marine biology, fisheries science, and ecological engineering around japan. *Fisheries Science*, *89*(2), 129–146.

Kuwatani, T., Kitao, K., Nishikawa, H., Tada, N., & Watanabe, H. K. (2023). Visualization of simulated paths of drifting pumices using point cloud PNG:towards the construction of hazard assessment system for drifting pumices (in Japanese with English Abstract). *Geoinformatics*, *34*(3), 61-68. doi: 10.6010/geoinformatics.34.3_61

Kuwatani, T., Nagao, H., Ito, S.-i., Okamoto, A., Yoshida, K., & Okudaira, T. (2018). Recovering the past history of natural recording media by bayesian inversion. *Physical Review E*, *98*(4), 043311.

Kuwatani, T., Nagata, K., Okada, M., & Toriumi, M. (2012). Precise estimation of pressure–temperature paths from zoned minerals using markov random field modeling: theory and synthetic inversion. *Contributions to Mineralogy and Petrology*, *163*, 547–562.

MacIntyre, R. (1966). Rapid growth in stalked barnacles. *Nature*, *212*(5062), 637–638.

Maeno, F., Kaneko, T., Ichihara, M., Suzuki, Y. J., Yasuda, A., Nishida, K., & Ohminato, T. (2022). Seawater-magma interactions sustained the high column during the 2021 phreatomagmatic eruption of Fukutoku-Oka-no-Ba. *Communications Earth & Environment*, *3*(1), 260.

Manga, M., Fauria, K. E., Lin, C., Mitchell, S. J., Jones, M. P., Conway, C. E., … Tani, K. (2018). The pumice raft-forming 2012 Havre submarine eruption was effusive. *Earth and Planetary Science Letters*, *489*, 49-58. doi: https://doi.org/10.1016/j.epsl.2018.02.025

Matsumura, T., Kuwayama, Y., Ueki, K., Kuwatani, T., Ando, Y., Nagata, K., … Nagao, H. (2021). Bayesian modeling of the equation of state for liquid iron in earth's outer core. *Journal of Geophysical Research: Solid Earth*, *126*(12), e2021JB023062.

Mesaglio, T. P., Schilling, H. T., Adler, L., Ahyong, S. T., Maslen, B., & Suthers, I. M. (2021). The ecology of lepas-based biofouling communities on moored and drifting objects, with applications for marine forensic science. *Marine Biology*, *168*, 1–16.

Metropolis, N., Rosenbluth, A. W., Rosenbluth, M. N., Teller, A. H., & Teller, E. (1953). Equation of state calculations by fast computing machines. *The journal of chemical physics*, *21*(6), 1087–1092.

Mitchell, S. J., Fauria, K. E., Houghton, B. F., & Carey, R. J. (2021). Sink or float: microtextural controls on the fate of pumice deposition during the 2012 submarine Havre eruption. *Bulletin of Volcanology*, *83*, 1–20.

Miyama, T. (2023). Simulation of drifting pumice from the fukutoku-oka-no-ba submarine volcano (in Japanese). *Journal of the Japan Society for Marine Surveys and Technology*, *35*(1), 19–21.

Mizutani, A., & Melgar, D. (2023). Potential volcanic origin of the 2023 short-period tsunami in the izu islands, japan. *Seismica*, *2*(2).

Morishige, M., & Kuwatani, T. (2020). Bayesian inversion of surface heat flow in subduction zones: a framework to refine geodynamic models based on observational constraints. *Geophysical Journal International*, *222*(1), 103–109.

Nakao, A., Kuwatani, T., Ito, S.-i., & Nagao, H. (2024a). Adjoint-based data assimilation for reconstruction of thermal convection in a highly viscous fluid from surface velocity and temperature snapshots. *Geophysical Journal International*, *236*(1), 379–394.

Nakao, A., Kuwatani, T., Ito, S.-i., & Nagao, H. (2024b). Adjoint-based marker-in-cell data assimilation for constraining thermal and flow processes from lagrangian particle records. *Authorea Preprints*.

Nishikawa, H., Kuwatani, T., Tada, N., & Kayama Watanabe, H. (2023). Simulated distributions of pumice rafts in Japan following eruptions at volcanic islands and submarine volcanoes. *Progress in Earth and Planetary Science*, *10*(1), 1–20.

Okubo, A. (1971). Oceanic diffusion diagrams. In *Deep sea research and oceanographic abstracts* (Vol. 18, pp. 789–802).

Omori, T., Kuwatani, T., Okamoto, A., & Hukushima, K. (2016). Bayesian inversion analysis of nonlinear dynamics in surface heterogeneous reactions. *Physical Review E*, *94*(3), 033305.

Putman, N. F., Goni, G. J., Gramer, L. J., Hu, C., Johns, E. M., Trinanes, J., & Wang, M. (2018). Simulating transport pathways of pelagic sargassum from the equatorial atlantic into the caribbean sea. *Progress in oceanography*, *165*, 205–214.

Sandanbata, O., Satake, K., Takemura, S., Watada, S., Maeda, T., & Kubota, T. (2024). Enigmatic tsunami waves amplified by repetitive source events near sofugan volcano, japan. *Geophysical Research Letters*, *51*(2), e2023GL106949.

Sandanbata, O., Watada, S., Satake, K., Kanamori, H., Rivera, L., & Zhan, Z. (2022). Sub-decadal volcanic tsunamis due to submarine trapdoor faulting at sumisu caldera in the izu–bonin arc. *Journal of Geophysical Research: Solid Earth*, *127*(9), e2022JB024213. doi: https://doi.org/10.1029/2022JB024213

Tada, N., Nishikawa, H., Ichihara, H., Watanabe, H. K., & Kuwatani, T. (2021). Drift of an ocean bottom electromagnetometer from the Bonin to Ryukyu Islands: estimation of the path and travel time by numerical tracking experiments. *Earth, Planets and Space*, *73*(1), 224.

Tamura, Y., Gill, J. B., Tollstrup, D., Kawabata, H., Shukuno, H., Chang, Q., ... others (2009). Silicic magmas in the izu–bonin oceanic arc and implications for crustal evolution. *Journal of Petrology*, *50*(4), 685–723.

Trinanes, J. A., Olascoaga, M. J., Goni, G. J., Maximenko, N. A., Griffin, D. A., & Hafner, J. (2016). Analysis of flight MH370 potential debris trajectories using ocean observations and numerical model results. *Journal of Operational Oceanography*, *9*(2), 126–138.

Van Sebille, E., Griffies, S. M., Abernathey, R., Adams, T. P., Berloff, P., Biastoch, A., ... others (2018). Lagrangian ocean analysis: Fundamentals and practices. *Ocean modelling*, *121*, 49–75.

Watanabe, K. H., Nagai, Y., Sakai, S., Kobayashi, G., Yamamori, L., Tada, N., ... Yusa, Y. (2024). Heterogeneous shell growth of a neustonic goose barnacle *Lepas anserifera*. *Marine Biology*, *171*(1), 161. doi: https://doi.org/10.1007/s00227-024-04481-8

Wessel, P., Smith, W. H., Scharroo, R., Luis, J., & Wobbe, F. (2013). Generic mapping tools: improved version released. *Eos, Transactions American Geophysical Union*, *94*(45), 409–410.

Yoshida, K., Tamura, Y., Sato, T., Hanyu, T., Usui, Y., Chang, Q., & Ono, S. (2022). Variety of the drift pumice clasts from the 2021 Fukutoku-Oka-no-Ba eruption, Japan. *Island Arc*, *31*(1), e12441.

Yuasa, M. (1995). Myojin knoll, Izu-Ogasawara arc : Submersible study of submarine pumice volcano. *Bulletin of the Volcanological Society of Japan*, *40*(4), 277-284. doi: 10.18940/kazan.40.4_277

Zheng, M., Mittal, T., Fauria, K. E., Subramaniam, A., & Jutzeler, M. (2022). Pumice raft detection using machine-learning on multispectral satellite imagery. *Frontiers in Earth Science*, *10*, 838532.

Estimating the Source of Floating Pumice Found near Torishima Island, Japan: A Back-Tracking Drift Simulation Approach

T. Kuwatani[1], H. Nishikawa[2], Y. Tanaka[2,3], H. K. Watanabe[4], N. Tada[1], A. Nakao[5,1], Y. Tamura[1], and S. Ono[1]

[1]Volcanoes and Earth's Interior Research Center (VERC), Research Institute for Marine Geodynamics (IMG), Japan Agency for Marine-Earth Science and Technology (JAMSTEC), 2-15 Natsushima-cho, Yokosuka, Kanagawa237-0061, Japan .
[2]Research Institute for Value-Added-Information Generation(VAiG), Japan Agency for Marine-Earth Science and Technology, 3173-25 Showa-machi, Kanazawa-ku, Yokohama, Kanagawa 236-0001, Japan
[3]Ocean Eyes Co., Ltd., Uradeyamacho 308, Nakagyo-ku, Kyoto-shi, Kyoto 604-8155, Japan
[4]Institute for Extra-Cutting-Edge Science and Technology Avant-Garde Research (X-Star), Japan Agency for Marine-Earth Science and Technology, 2-15 Natsushima-cho, Yokosuka, Kanagawa237-0061, Japan
[5]Graduate School of Engineering Science, Akita University, Akita 010-8502, Japan

Key Points:

- A back-tracking drift simulation was conducted for floating pumice discovered on October 20, 2023, near Torishima Island in the Izu Islands
- The pumice drifted southward and originated from around back-arc basins near Myojinsho Reef and Sumisujima Island about 3–5 days before
- Results are consistent with petrology, biology, and geochemistry studies and suggest an unknown pumice source

Corresponding author: Tatsu Kuwatani, `kuwatani@jamstec.go.jp`

Abstract

Monitoring and detecting marine volcanic activities are key for scientific understanding and disaster prevention. However, this is difficult because they are hidden under water. Near Torishima Island in the Izu Islands, Japan, intensified seismic activity was observed during October 2023, including a mysterious tsunami-triggering earthquake on October 8 (UTC), which was considered to be linked to a volcanic activity. On October 20, 2023, aerial surveys confirmed an 80-km stretch of floating pumice near Torishima Island. This study conducted a Lagrangian back-tracking drift simulation using the ocean current data and surface wind data to trace the origin of the pumice while clarifying the theoretical basis of Lagrangian back-tracking from the Bayesian perspective. Results indicate that the pumice drifted southward from around extensional back-arc basins near Myojinsho Reef and Sumisujima Island approximately 3–5 days before its discovery. These findings are consistent with independent observations such as biological traces and the geochemical characteristics of sampled floating pumice, which is considered identical to that found on October 20 by an airplane. This indicates the presence of unknown volcanic activity around back-arc basins west of the major active volcanic zone. This study demonstrates the utility of combining drift simulations with geochemical and biological data to identify the sources of marine volcanic events, particularly in regions where direct observations are limited. The results of this study contribute to our understanding of volcanic mechanisms and their potential hazards.

Plain Language Summary

In October 2023, volcanic pumice was found floating over a large area of the ocean near Torishima Island, part of the Izu Island chain, Japan. This occurred during a period of increased seismic activity near Torishima Island, including an earthquake that caused a tsunami, with no clear explanation of its mechanism. We conducted a computer simulation using ocean current data to trace the journey of this pumice backward in time to determine its source. The results of this study suggest that the pumice originated from an unknown underwater volcanic eruption that occurred 3–5 days before the discovery of the floating pumice. The eruption likely occurred around a underwater basin region, which is an area where the Earth's crust is being pulled apart, allowing magma to reach the ocean floor. Our research shows the effectiveness of using such simulations to trace the origins of floating pumice and to identify hidden underwater volcanic activities. Such simulations add to our understanding of the complexities of underwater volcanic activities and their potential hazards.

1 Introduction

Understanding marine volcanic activity, including submarine volcanoes and volcanic islands, and elucidating their formation mechanisms, as well as predicting their activity, are important in academic fields and for disaster prevention and mitigation. However, marine volcanoes are commonly located in remote areas and are hidden under water. Hence, directly observing and monitoring such volcanoes even by geophysical observations and remote sensing are difficult. Therefore, it is challenging to determine the location, scale, and duration of marine volcanic activity.

In the ocean near Torishima Island in the Izu Island chain (Figure 1), seismic activity intensified after October 2, 2023. According to observations by the Japan Meteorological Agency (JMA), four earthquakes with a magnitude (M) of 6.0 or higher were recorded up to October 9. Furthermore, numerous earthquakes occurred after 4:00 A.M. on October 9, including small earthquakes with undetermined epicenters (Japan Meteorological Agency, 2023a). Despite the magnitude of these earthquakes being smaller than those typically expected to generate tsunamis, tsunamis were observed along the Pacific coasts of the Izu–Bonin Islands, Chiba Prefecture, Shikoku, and Kyushu Islands. The mechanisms and causes of these seismic activities and tsunamis, which are potentially related to volcanic activities, are not well understood. Various investigations, including seismological observations, physical exploration, and marine surveys using research vessels, are currently underway to elucidate the details and mechanism of these geological events and to monitor the evolving situation. Additionally, numerous rapid reports were released by organizations such as the National Institute of Advanced Industrial Science and Technology (AIST), Earthquake Research Institute (ERI) at the University of Tokyo, Japan Agency for Marine-Earth Science and Technology (JAMSTEC), and JMA (AIST, 2023a, 2023b; ERI, U Tokyo, 2023; JAMSTEC, 2023a, 2023c, 2023d; Japan Meteorological Agency, 2023b). Recent geophysical studies have clarified the details of earthquakes, revealing that they occurred around Sofu seamount caldera located 20–30 km west of the Sofugan Rock (Fig. 1(b)) (Mizutani & Melgar, 2023; Sandanbata et al., 2024; Kubota et al., 2024; Fujiwara et al., 2024).

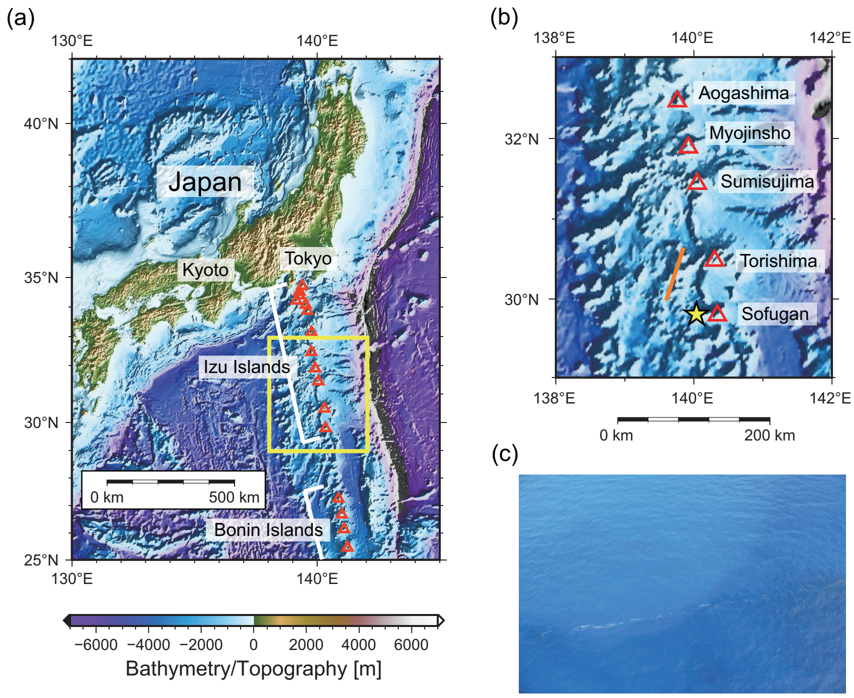

Figure 1. Bathymetric maps of the study area. (a) Japan and the northern part of the Izu–Bonin arc. Red triangles represent active volcanoes in the Izu–Bonin arc, listed by the JMA. (b) Enlarged map of the southern Izu Islands (within yellow framework shown in [a]). Orange line indicates the distribution of the floating pumice observed by the Japan Coast Guard's observation airplane on October 20, 2023 (Japan Coast Guard, 2023b). The location of Sofu seamount is indicated by yellow star. The bathymetric map is based on ETOPO1 (Amante & Eakins, 2009). (c) Floating objects observed by the Japan Coast Guard's observation airplane (shot at 14:25 (JST) October 20, 2023) (Japan Coast Guard, 2023b).

On October 20, 2023, a Japan Coast Guard observation airplane confirmed the presence of pumice floating in the sea scattered over approximately 80 km in a north–south direction about 50 km west of Torishima Island (from 30°41'N, 139°51'E to 29°59'N, 139°36'E) (Japan Coast Guard, 2023b) (Fig. 1). Maritime warnings were issued, and vessels in the vicinity were alerted. An expert noted that there were no recognized active volcanoes in this area, suggesting the possibility of new volcanic activity and, potentially, the formation of a submarine volcanic body. Subsequently, the JMA's research vessel "KEI-FUMARU" collected pumice samples (Japan Meteorological Agency, 2023b), and preliminary petrological descriptions and geochemical analyses were reported (AIST, 2023a, 2023b; ERI, U Tokyo, 2023). These reports suggested that one type of pumice samples may be a part of the same pumice raft. This will be discussed in detail in the Discussion section. However, pumice rafts were not detected in the satellite imagery in the nearby area during this period, and we could not find any evidence in publicly available satellite imagery data including Sentinel.

Drift pumice is often found washed up on coasts. According to Bryan et al. (2004), massive drifts of pumice occur globally every few to several decades. In recent years, significant pumice raft drifting events have occurred, including the 2012 eruption of the Havre Volcano in the Tonga–Kermadec Arc (Jutzeler et al., 2014), the 2019 eruption of the Tonga F Volcano (Jutzeler et al., 2020), and the 2021 eruption of the Fukutoku-Oka-no-Ba submarine volcano (e.g. Tada et al., 2021; Yoshida et al., 2022; Maeno et al., 2022; Fauria et al., 2023). These pumice rafts pose hazards to maritime traffic, fisheries, tourism, and local ecosystems (Jutzeler et al., 2014, 2020). They also serve as crucial physical evidence for understanding the eruption mechanisms of submarine volcanoes, and various studies have been conducted on the formation, floating, and sinking mechanisms and drifting phenomena of pumice produced by submarine volcanic eruptions (e.g. Fauria et al., 2017; Kano, 2003; Cas & Simmons, 2018; Mitchell et al., 2021; Yoshida et al., 2022; Knafelc et al., 2022).

Forward drift simulations, in which a large number of virtual particles are moved in accordance with the flow fields of ocean currents, are effective for predicting the spatial dispersal of pumice. Previous research using drift simulations for predicting the distribution of pumice rafts focused on a previously unknown volcano (0403-91) (Bryan et al., 2004) and Home Reef volcano eruptions (Bryan et al., 2012) along the Tonga arc, the 2012 Havre Volcano eruptions (Jutzeler et al., 2014), and the 2019 Tonga F Volcano eruptions (Jutzeler et al., 2020). Several drift simulations focusing on the pumice drift caused by the 2021 eruption of the Fukutoku-Oka-no-Ba submarine volcano were conducted (Chang et al., 2023; Iskandar et al., 2023; Miyama, 2023). In addition to these studies that simulated actual drift events, forward drift calculations have been conducted for hazard and risk preassessment purposes, assuming eruptions of various submarine volcanoes near Japan (Nishikawa et al., 2023; Kuwatani et al., 2023). Moreover, using simulation results, a preliminary report about the future drift of pumice discovered near Torishima Island was submitted to agencies responsible for volcanic disaster prevention (JAMSTEC, 2023b).

Drift simulations can be used not only for predictions but also for back-tracking estimations (e.g. Van Sebille et al., 2018; Kuroda, 2023). In particular, several research groups conducted back-tracking simulations to estimate the crash location of Malaysia Airlines Flight MH370, which went missing in flight in 2014, based on debris found around the Indian Ocean from 2015 to 2016 (Jansen et al., 2016; Trinanes et al., 2016; Al-Qattan et al., 2023). In addition, our group conducted a back-tracking simulation to estimate the drift start time and path of an ocean bottom electromagnetometer that had been installed on the seafloor of the Nishinoshima Volcano in the Ogasawara Islands and went missing in 2019 (Tada et al., 2021). It was found on the coast of Iriomote Island in the Ryukyu Islands, more than 1,700 km away from the Ogasawara Islands, in February 2021. This research enabled the immediate provision of information to relevant organizations following the eruption of the Fukutoku-Oka-no-Ba submarine volcano in 2021, as we had been studying pumice drifting from the Ogasawara Islands to the Ryukyu Islands and its potential hazards. In addition, Tada et al. (2021) preliminarily mentioned the possibility of exploring unknown submarine volcanoes as a source of pumice, as was conducted in the current study.

This study had two primary objectives: to provide independent insights that contribute to understanding the series of enigmatic geological events occurred near Torishima Island in 2023 and to evaluate the utility of drift simulations in understanding and monitoring submarine volcanic activities. To achieve these objectives, a back-tracking drift simulation using the ocean current data was conducted to estimate the source of the floating pumice discovered near Torishima Island on October 20, 2023, while clarifying the theoretical basis of the back-tracking simulation. The results are compared with other studies that have employed independent approaches (i.e., biological traces and geochemical studies). The connection of the floating pumice to the seismic activity near Torishima Island since October, including the tsunami event occurred on October 9, is also explored. The discussion further includes methodological observations on Lagrangian back-tracking simulations, submarine volcanic activity, and directions for the future research.

2 Back-Tracking Simulation Using Ocean Re-analysis Data

In this section, we initially present a simple theoretical foundation for back-tracking numerical experiments, which have been empirically applied in many studies, using the framework of the Bayesian inversion analysis. We then describe the problem settings and parameters assumed for the drift simulation of the 2023 Torishima floating pumice and present the simulation results.

2.1 Method

Lagrangian data analyses or particle tracking simulations are often used for analyzing floating or suspended organisms and particles in the ocean (e.g. Van Sebille et al., 2018; Kuroda, 2023). The random-walk motion of a Lagrangian particle in a velocity field can be simply expressed using the advection and diffusion terms as follows:

$$\boldsymbol{x}_{t+|\Delta t|} = \boldsymbol{x}_t + \boldsymbol{u}(\boldsymbol{x}_t, t) \cdot |\Delta t| + \sqrt{2D \cdot |\Delta t|} \cdot \boldsymbol{\xi}_{\mathcal{N}}, \tag{1}$$

where $\boldsymbol{x}_t$ is the particle position at time step t; $\boldsymbol{u}(\boldsymbol{x}, t)$ is the velocity field vector at position $\boldsymbol{x}$ and time t; $|\Delta t|$ is a small interval of the time step; D is the diffusion coefficient of the random walk; and $\boldsymbol{\xi}_{\mathcal{N}}$ is a random-number vector in which each element indicates the standard normal distribution. The last term of the right-hand equation represents diffusion due to the random-walk motion, where the standard deviation σ equals $\sqrt{2D \cdot |\Delta t|}$. Because the diffusion process is irreversible, Eq. (1) holds only in the forward time direction. To clearly distinguish between the forward and backward times directions, the absolute value $|\Delta t|$ is used to represent the time step. Equation (1) provides a general and simple formulation for representing the Lagrangian particle motion and is widely used in various natural science fields, including ocean modeling.

Because Eq. (1) represents an irreversible diffusion process, it cannot be directly used for the back-tracking simulation by reversing the sign of either the velocity field $\boldsymbol{u}$ or Δt. In this study, using the Bayesian framework, we try to estimate the past position of the particle from the present position. Bayesian estimation is based on the posterior probability, which is the probability of unknown estimates for a given observable or known values. Using Bayes' theorem, the posterior probability of the one-step-back past position $\boldsymbol{x}_{t-|\Delta t|}$ that yields the present position $\boldsymbol{x}_t$ can be written as follows:

$$p\left(\boldsymbol{x}_{t-|\Delta t|} \mid \boldsymbol{x}_t\right) \propto p\left(\boldsymbol{x}_t \mid \boldsymbol{x}_{t-|\Delta t|}\right) \cdot p\left(\boldsymbol{x}_{t-|\Delta t|}\right), \tag{2}$$

where $p\left(\boldsymbol{x}_t \mid \boldsymbol{x}_{t-|\Delta t|}\right)$ is a likelihood function that can be represented by a general type of probabilistic physical models in the forward time direction and $p\left(\boldsymbol{x}_{t-|\Delta t|}\right)$ is a prior probability using which our prior knowledge regarding the past position can be incorporated into the analysis.

The Lagrangian particle motion equation (Eq. 1) can be directly used as the likelihood function by only shifting one time step backward as $t \to t - |\Delta t|$. Specifically, the likelihood function indicates that $\boldsymbol{x}_t$ shows the Gaussian distribution with a mean of $\bar{\boldsymbol{x}}_t = \boldsymbol{x}_{t-|\Delta t|} + \boldsymbol{u}(\boldsymbol{x}_{t-|\Delta t|}, t)\Delta t$ and variance of $\sigma^2 = 2D \cdot |\Delta t|$. Furthermore, we assume that the prior probability $p\left(\boldsymbol{x}_{t-|\Delta t|}\right)$ has a continuous uniform distribution, in which case there is no useful prior knowledge about the past.

By substituting these expressions into the likelihood function $p\left(\boldsymbol{x}_t \mid \boldsymbol{x}_{t-|\Delta t|}\right)$ and prior probability $p\left(\boldsymbol{x}_{t-|\Delta t|}\right)$ in Eq. (2), the posterior distribution of the previous step is given by

$$p\left(\boldsymbol{x}_{t-|\Delta t|} \mid \boldsymbol{x}_t\right) \propto \exp\left(-\frac{||\boldsymbol{x}_{t-|\Delta t|} - (\boldsymbol{x}_t - \boldsymbol{u}(\boldsymbol{x}_{t-|\Delta t|}, t) \cdot |\Delta t|)||^2}{4D \cdot |\Delta t|}\right). \tag{3}$$

Using this equation, we can probabilistically estimate the previous position $\boldsymbol{x}_{t-|\Delta t|}$ from the present position $\boldsymbol{x}_t$ as a normal distribution with a mean of $\boldsymbol{x}_t - \boldsymbol{u}(\boldsymbol{x}_{t-|\Delta t|}, t) \cdot |\Delta t|$ and variance of $\sigma^2 = 2D \cdot |\Delta t|$. Similar to considering the Lagrangian particle motion equation (Eq. 1) as a probability when substituted to the likelihood function, the posterior probability (Eq. 3) can be directly reversed to a virtual Lagrangian particle motion equation as follows:

$$\boldsymbol{x}_{t-|\Delta t|} = \boldsymbol{x}_t + \boldsymbol{u}_{\text{rev}}(\boldsymbol{x}_t, t) \cdot |\Delta t| + \sqrt{2D \cdot |\Delta t|} \cdot \boldsymbol{\xi}_{\mathcal{N}}, \tag{4}$$

where $\boldsymbol{u}_{\text{rev}}(\boldsymbol{x}_t, t)$ is a reversed velocity field defined as $\boldsymbol{u}_{\text{rev}}(\boldsymbol{x}_t, t) \equiv -\boldsymbol{u}(\boldsymbol{x}_t, t)$. When deriving the above equation, we used the approximation $\boldsymbol{u}(\boldsymbol{x}_{t-|\Delta t|}, t) \sim \boldsymbol{u}(\boldsymbol{x}_t, t)$, which holds in a natural situation where $|\Delta t|$ is sufficiently small and the velocity field does not change abruptly in time and space. Equation (4) is similar to the motion equation that has been empirically used in Lagrangian back-tracking simulations.

2.2 Experimental Settings

Using Eq. (4), we conducted a back-tracking drift simulation of Lagrangian particles to trace back the possible pathways of floating pumices from the region from which they were found (Fig. 1(b)). In this study, the pumice is assumed to horizontally move on the sea surface so that its position $\boldsymbol{x}_t$ indicates a horizontal location, which comprises east–west and north–south coordinates at time t. The horizontal movement of the pumice is known to be driven by a combination of ocean currents, windage, and waves (e.g. Bryan et al., 2004; Jutzeler et al., 2014). Ocean currents and windage are incorporated into the reverse velocity vector field ($\boldsymbol{u}_{\text{rev}}(\boldsymbol{x}, t)$) in the advection term. Furthermore, the effect of waves is included in the diffusion term ($+\sqrt{2D \cdot |\Delta t|} \cdot \boldsymbol{\xi}_{\mathcal{N}}$).

The effect of surface winds on the pumice movement remains a subject of debate in several studies (Jutzeler et al., 2020; Chang et al., 2023; Iskandar et al., 2023; Chiang et al., 2024). In this study, the following four cases are considered for analyzing the effect on the velocity field: no wind effect (0%) and the addition of 1%, 3%, and 5% of the surface wind speed to the velocity field of the ocean current. These windage values are consistent with recent studies: 1–4 % used for the 2019 Tong F pumice (Jutzeler et al., 2020) and 0–2 % (Chang et al., 2023), 2-3% (Iskandar et al., 2023), and 3% (Chiang et al., 2024) for the 2021 Fukutoku-Oka-no-Ba pumice. In addition, our values are consistent with previous simulations for other floating objects, for example, 0 and 1 % employed for a study on pelagic *Sargassum* (Putman et al., 2018) and 0 % for an ocean bottom electromagnetometer (Tada et al., 2021).

The reverse velocity vector field ($\boldsymbol{u}_{\text{rev}}(\boldsymbol{x}, t) \equiv -\boldsymbol{u}(\boldsymbol{x}, t)$) comprises the eastward and northward velocities at position $\boldsymbol{x}$ and time t and is given by the negative of combination of ocean currents and windage (0%, 1%, 3%, and 5% surface wind speed). For ocean currents, we used horizontal velocity obtained from an ocean re-analysis dataset provided for operational numerical weather prediction by Japan Meteorological Agency (2013a). This is daily data, and their horizontal resolution is 0.02° × 0.030303° (2.23 km × 2.89 km) for latitude and longitude, respectively. For surface wind, we used the wave-speed dataset based on the meso-scale model (MSM) reported by JMA (Japan Meteorological Agency, 2024). This is daily data, and their horizontal resolution is 0.05°× 0.0625° (5.57 km × 5.96 km) for latitude and longitude, respectively. The diffusion term $(+\sqrt{2D \cdot |\Delta t|} \cdot \boldsymbol{\xi}_{\mathcal{N}})$ indicates horizontal diffusion, which comprises east–west and north–south components, each of which is generated by the standard normal distribution. This term is derived from two probabilistic causes: one is a random Brownian motion of particles, called horizontal eddy diffusion, resulting from waves, wind, and other forces in the natural system, and the other is uncertainty. In this study, we set diffusion coefficient D at 10 m^2 s^{-1} based on the general value of horizontal eddy diffusion for small to meso-scale processes (e.g. Okubo, 1971). Note that the equation for particle back-tracking (Equation 4) and the diffusion coefficient are the same as those reported in Tada et al. (2021).

In each experiment, we used 2,600 particles (100 particles at each 26 initial position spaced according to the horizontal resolution of the ocean re-analysis dataset), with the region where the pumice was observed (Fig. 1(b)) being the initial condition. Particles are assumed to move at a depth of 1 m, which corresponds to the shallowest depth in the ocean re-analysis dataset and are released at 00:00 UTC on October 20, 2023. The particles are tracked hourly for 30 days, with the time step $|\Delta t|$ set to 20 min.

2.3 Results

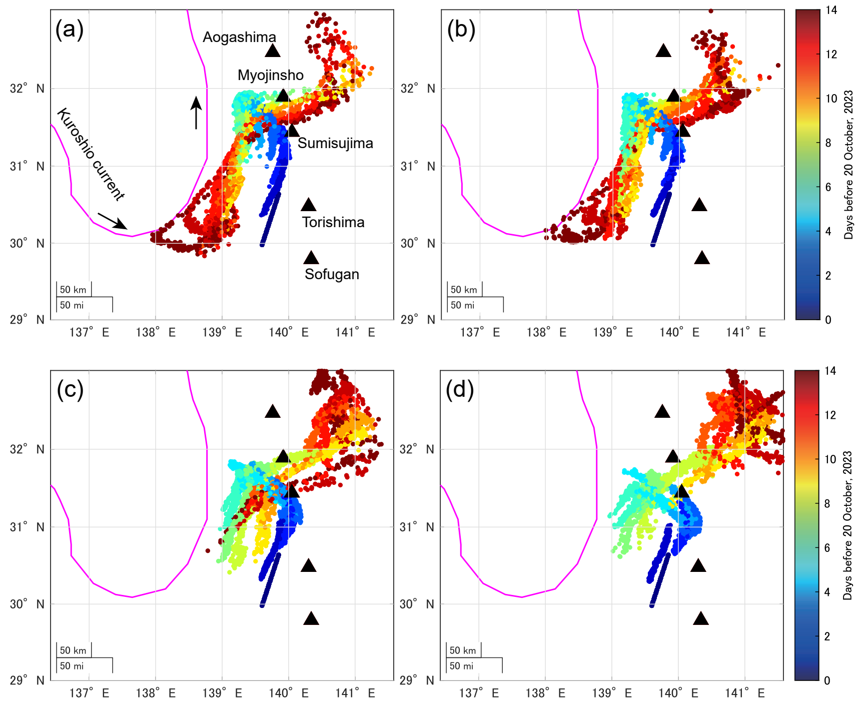

Figure 2. The spatial distribution of particle locations obtained from the back-tracking simulations show each day's distribution. The pseudocolors indicate the number of days the particles were traced back from the start of the drift back-tracking on October 20, 2023 (UTC). Particle locations were traced back for up to 14 days without the effect of wind (a) and with 1% (b), with 3% (c), and (d) 5% effect of wind. Magenta line in each panel represents the Kuroshio Current streamlines during October 10—17, and these data are provided by Japan Coast Guard (2023a).

Figures 2 (a), (b), (c), and (d) show the results of particle tracing back at 0 %, 1%, 3%, and 5% windage, respectively, for up to 14 days. Videos showing the dispersal of the particle distribution over time in the forward and backward time directions for 30 days is available in Supplementary Materials. By comparing the time evolution of the spatial pattern across different cases, they can be classified into two main categories: the weak windage cases (0% and 1%), where windage has no or a negligible effect, and strong windage (3% and 5%), where windage has a significant impact. Below, the temporal change in the spatial pattern is explained for each category. Unless otherwise noted, the explanation will be in the direction of tracing back in time.

For the weak windage (0% (without wind) and 1%) cases (Figure 2(a,b)), in a time-reversed direction, particles initially moved northward, passing west of Sumisujima Island around October 17, and then changed course toward northwest. Around October 14, near the west side of Myojinsho Reef, they started to significantly disperse in the southwest and easterly directions. After the split around October 7, particles that entered the southwest side of Myojinsho Reef were approximately aligned with the Kuroshio Current axis and rode this faster current along its axis, moving up to the vicinity of Kyushu Island within 30 days (refer to Supplementary Materials). Those that moved eastward initially reached the east of the volcanic front and then moved northward near Hachijojima; then, a large portion of the particles rode the Kuroshio Current and moved westward (see the Supplementary Materials).

For 3% and 5% windage cases (Figure 2(c,d)), particles initially moved northward, similar to the weak windage effect cases. They also passed the vicinity area of Sumisujima Island around October 17 and then changed course toward northwest. As the effect of the windage increased, particles tended to take a more easterly path (the front-arc side). Although they moved to the western region of Myojinsho Reef, they were pushed back to a slightly more Southerner area, compared with the weak windage cases. Around October 14, they began to disperse in the southwest and easterly directions. However, they did not split two parts, unlike in the weak windage cases, and most particles moved in the northeast direction and reached the east side of the volcanic front. After drifting in that area for several days, a group of particles rode the Kuroshio Current near Hachijojima and moved westward with the current, similar to the weak windage case. After the ride, particles might escape the Kuroshio Current relatively easily, unlike the weak windage cases (see Supplementary Materials). In fact, a part of particles sometimes moved in the east direction, which might have been caused by the effect of strong windage that might have continued from hours to days, and they came back to the Izu Islands area.

Figure 3 shows the ocean current velocity field on October 15 (UTC). Near N32°, E138°, west of the Myojin Reef, there is a collision point where an east-to-west current collides with the northward-flowing Kuroshio Current. From the southeastern corner of this point, an ocean current flows southward along the west side of the Izu Islands. Particle movements near the discovery date can be interpreted in the forward time direction based on the spatial pattern of the ocean current as follows. In the weak windage cases, two groups of particles emerged: particles that followed the northward Kuroshio Current and those that rode the east-to-west current from the front-arc to the back-arc side. These groups converged near the collision point west of Myojinsho Reef and then moved southward toward the discovery area near Torishima, riding the southward Kuroshio countercurrent. In the strong windage case, all particles moved through the Myojinsho Reef area by riding the east-to-west current and then traveled southward by riding the Kuroshio countercurrent to the discovery area near Torishima .

The overall movement of particles was predominantly governed by stable and consistent ocean currents, which persisted in the same locations over extended periods. In contrast, the wind field, which tends to fluctuate in terms of the direction and speed over short periods, exerted perturbative influences on the particles' movement, particularly during strong windage events. The extent of this impact depended on the intensity of the windage. Differences in the particle behavior between the weak and strong windage cases likely stemmed from the windage effect from the northeast direction. In the strong windage case, the windage likely impeded the inflow of particles from the Kuroshio Current.

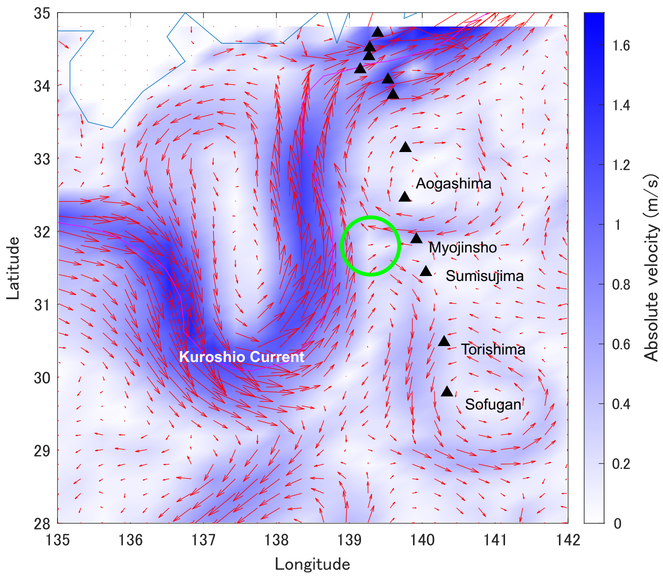

Figure 3. Ocean current patterns on October 15 at 00:00 (UTC). The Kuroshio Current axis is based on the numerical information published by the Japan Coast Guard's Oceanographic Information Division. `https://www1.kaiho.mlit.go.jp/KANKYO/KAIYO/qboc/kurosio-num.html` Green circle indicates a southeastern corner of the collision point where an east-to-west current collides with the northward-flowing Kuroshio Current.

3 Estimating the Spatial and Temporal Source of the Floating Pumice

3.1 Method

By assuming that all pumice particles originated from a single event, we try to estimate the time and location of the pumice origin. This assumption aligned with our intuition that it was unlikely (although not impossible) for pumice widely scattered across the Pacific to have coincidentally gathered. When assuming that the pumice originated from a single event, the following condition is likely to be met: the initial pumice distribution near the source should be concentrated in a narrow region. In other words, we expect to identify a time and location that satisfy this condition to some extent. Here, we evaluate the concentration at a given time t by the spread of distances from the centroid of the point cloud as follows:

$$S(t) = \sqrt{\frac{d_{\mathrm{lon}}^2}{N}\sum_{n=1}^{N}\left(x_{\mathrm{lon},n}(t) - \bar{x}_{\mathrm{lon}}(t)\right)^2 + \frac{d_{\mathrm{lat}}^2}{N}\sum_{n=1}^{N}\left(x_{\mathrm{lat},n}(t) - \bar{x}_{\mathrm{lat}}(t)\right)^2}, \tag{5}$$

where $x_{\mathrm{lon},n}(t)$ and $x_{\mathrm{lat},n}(t)$ are the longitude and latitude of a particle n for time t, respectively; $\bar{x}_{\mathrm{lon}}(t)$ and $\bar{x}_{\mathrm{lat}}(t)$ are the mean values of the longitude and latitude, respectively;N is the total number of particles, and d_{lon} and d_{lat} are the coefficients used to convert differences in the longitude and latitude into distances, respectively. We used 95.42 and 111.32

km for 1° by assuming a latitude of around 31°N. A larger $S(t)$ indicates a lower concentration, whereas a smaller $S(t)$ indicates a higher concentration.

In addition to the pumice concentration, we monitored isotropy as the initial pumice distribution around the source is expected to be isotropic to some extent rather than highly elongated in cases where the pumice raft spans more than several kilometers. For isotropy, we calculated the aspect ratio $\alpha(t)$ from the ratio of the eigenvalues obtained by the eigenvalue decomposition of the covariance matrix of the point cloud coordinates.

$$\alpha(t) = \sqrt{\lambda^{\mathrm{I}}(t)/\lambda^{\mathrm{II}}(t)}, \tag{6}$$

where $\lambda^{\mathrm{I}}(t)$ and $\lambda^{\mathrm{II}}(t)$ represent the larger and smaller eigenvalues at time t, respectively. An aspect ratio closer to 1 indicates isotropy, whereas a ratio closer to 0 indicates a highly elongated, straight-line distribution.

3.2 Results

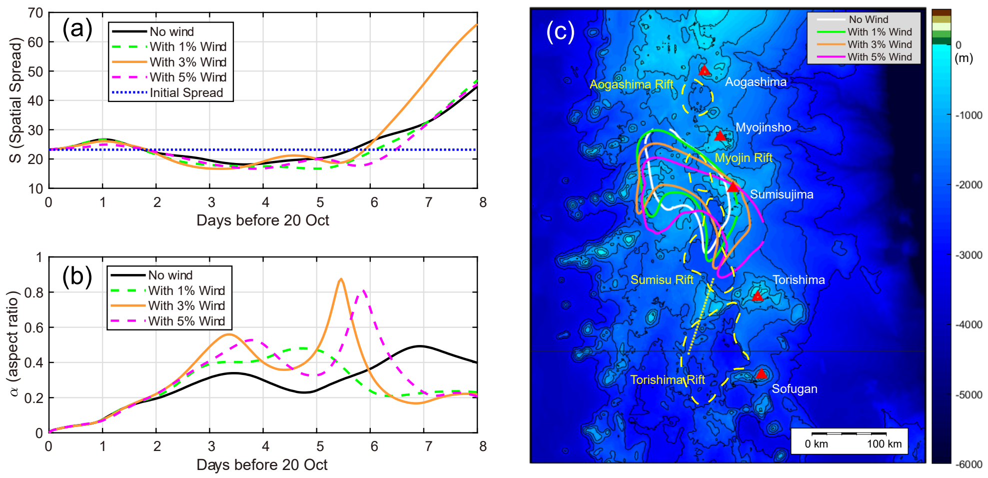

Figure 4. Results of the pumice source estimation. The time evolution of the spatial spread (a) and aspect ratio (b) are shown as time progresses backward from 00:00 on October 20 (UTC), corresponding to the discovery of the floating pumice. In (a), blue dotted line represents the initial spread value, which serves as the criteria for identifying a small spread value. (c) Spatial distribution of pumice particles when the spread is lower than the initial distribution observed on October 20. Using kernel density estimation, a contour line representing the 95% credible region is shown for each case: without wind effect (white) and 1% (green), 3% (orange), and 5% (magenta) wind. In (c), the initial positions of particles and active volcanoes are marked by small yellow circles and red triangles, respectively. The location of the Sofu seamount is indicated by a white star, and back-arc rifts are shown by yellow dashed lines.

Figures 4(a) and (b) show the temporal evolution of the spread $S(t)$ and the aspect ratio $\alpha(t)$, respectively. Regardless of the effect of windage, the spread initially increased slightly and then decreased as time was traced back from the discovery of the floating pumice. It then bottomed out at around 89 h (3 days and 17 hours) for without wind case and at 120 h (5 days) for 1% wind case, 78 h (3 days and 6 hours) for 3%

wind case, and 94 h (3 days and 22 hours) for 5% wind case. Subsequently, all cases exhibited a monotonically increasing trend with a steep slope from around 5–7 days. For all cases, the aspect ratio initially started from zero as it is distributed in a straight line, which is a simplified representation of the pumice observed on October 20, and exhibited the first peak around 3–5 days. It demonstrated distinct second peaks around 5–7 days for the 0%, 3%, and 5% cases, while it did not increase so largely for the 1% windy case.

Because the spread did not show a distinct minimum value in each case, identifying the source timing at the hour or one-day scale was difficult. However, it was considered to be around 3–5 days for all cases based on the time at which the spread exhibited a low value, similar to the minimum value for each case. The spread and aspect ratios showed extreme values (the first peak) at a similar time for each case. The source region was assumed to be the area with a dense particle distribution when the spread $S(t)$ is at its lowest.

Figure 4(c) shows the estimated source region overlaid on the seafloor topography. As mentioned earlier, the spread values did not display distinct minima in any of the cases; instead, they exhibited similar values over several days. To establish uniform and objective criteria while minimizing the risk of missing the source region and avoiding over interpretation, we set the threshold as inclusively as possible: the source timing was defined as the period when the spread values are smaller than the initial observed value and source region corresponded to an area containing 95% of particles. The estimated source regions were generally located on the back-arc side, including the northern part of the Sumisu Rift, Myojin Rift, and Sumisu Caldera. In the stronger windage cases, there was a slight shift toward the fore-arc side and southern regions, in comparison to the weaker windage cases.

4 Discussion

4.1 Lagrangian back-tracking simulation

Note that the Lagrangian back-tracking equation (Eq. 4) cannot either be interpreted as an equation of motion in the real physical world nor can it be physically and mathematically derived from the original forward Lagrangian equation alone properly. However, it can be regarded as an equation of motion for a virtual particle used in the probabilistic estimation of the past position in inversion analysis and can be properly derived through the Bayesian framework. Such a probabilistic particle representation is commonly employed in many inversion problems, such as in the Markov chain Monte Carlo algorithm (e.g. Metropolis et al., 1953; Gilks et al., 1995), and has been widely applied in Earth material sciences (e.g. Kuwatani et al., 2012; Morishige & Kuwatani, 2020; Matsumura et al., 2021).

Furthermore, probabilistic particle expressions for the time evolution of unknown variables are employed in data assimilation through sequential Monte Carlo algorithms, also known as particle filters, (e.g. Kitagawa, 1987; Doucet et al., 2000), and have been applied to Earth material sciences (e.g. Omori et al., 2016; Kuwatani et al., 2018; Ito et al., 2021). In adjoint-based data assimilation, used to estimate past states following an advection-diffusion equation, the diffusion term (with its sign reversed relative to the normal advection term) also appears in an adjoint equation for backward calculations, similar to Eq. (4). Ismail-Zadeh et al. (2004) demonstrated that this inverted diffusion term is necessary to accurately estimate a diffusive physical variable, such as heat, in a past state. Therefore, Eq. (4) can be seen as an approximate representation of the uncertainty in estimating particle positions, which increases as we move backward in time, and manifests as a diffusion term from a macroscopic view.

Although we adopted the Lagrangian particle simulation approach to trace the backward paths of the pumice in this study, we did not exclude the possibility of using other approaches to estimate past particle positions. Recently, we have developed advanced adjoint-based data assimilation methods that integrate Eulerian and Lagrangian perspectives to estimate the past state from the present state of the Earth's interior (Nakao et al., 2024a, 2024b). Further development of these methods may allow for the more precise estimate of particle trajectories compared with using only the Lagrangian method and also provide insights into reconstructing macroscopic velocity fields in which particles move.

4.2 Origin of the Pumice

The results of the back-tracking simulation suggest that the floating pumice drifted southward from the back-arc rift area located west of active volcanic fronts, such as Myojinsho Reef and Sumisujima Island, finally arriving at the position where it was found on October 20. This leads to the natural conclusion that the drifting pumice found near Torishima Island on October 20 via the airplane observation is unlikely to be directly related to a seismic activity near Torishima Island; more specifically, it is not related to Sofu seamount that occurred in October, particularly the earthquake event on October 8 (UTC) that caused an unexplained tsunami, which is considered to be related to a submarine volcanic activity. Instead, it seems likelier that they have different origins.

Because it is unlikely that the pumice originally spread over a wide area and coincidentally gathered, its source is presumed to have appeared after October 15 when particles began to widely disperse in the time-reverse direction under the influence of the Kuroshio Current and east-to-west current (Figure 2). Our analysis of the concentration and aspect ratio of the simulated particle cloud indicates that areas including the Myojin Rift, Sumisu Rift, and Sumisu caldera are reasonable source regions. The area east of the presumed source area, Bayonnaise Rocks including Myojinsho Reef, is located on a volcanic front, which is part of an active caldera, the Myojinsho caldera; additionally, several eruptions have occurred here over the past century, often accompanied by the formation and disappearance of islands (Japan Meteorological Agency, 2013b). In 1953, a research vessel encountered an eruption in this area, leading to a tragic incident in which 31 crew members lost their lives, and a tsunami was also observed. Eruption warnings have been continuously issued around Bayonnaise Rocks (Myojinsho Reef) since January 26, 2023 based on discolored water. Furthermore, Sumisu caldera also generates tsunamis approximately once every ten years caused by subsidence through trapdoor faults (Sandanbata et al., 2022).

In the extensional back-arc basins, called the back-arc rift zone, which is included by the estimated source of the pumice in this study, there is no direct evidence for the presence of active volcanoes. Deep-sea drilling in the Sumisu Rift has shown that the upper layers of sediment predominantly consist of pumice, suggesting submarine calderas or back-arc rifts as primary sources (Fujioka, 1989). Moreover, near the Myojin Knoll, located just east of the back-arc rift (approximately 40 km south of Aogashima and about 25 km north of the Bayonnaise Rocks), diving surveys by "Shinkai 2000" have confirmed that the caldera walls are composed of pumice. These surveys have also identified blocks of pumice larger than 1 m (Yuasa, 1995) on the seafloor.

The observed pumice raft area was roughly estimated to be 0.1–1 km^2 based on its length of about 80 km reported by (Japan Coast Guard, 2023b) and width of about 1–10 m roughly estimated by visualizing the photo Japan Coast Guard (2023b). The estimated area was considerably less than the recent reports of the actually observed area of the pumice raft: 1,600 km^2 for the 2006 Home Reef Volcano in Tonga (Bryan et al., 2012), 400 km^2 for the 2012 Havre eruption (Jutzeler et al., 2014), 195 km^2 for the 2019 Tonga F eruption (Jutzeler et al., 2014), and 290 km^2 for Fukutoku-Oka-no-Ba (Ikegami, 2021). The pumice found near Torishima was likely too minor to be detected via routine satellite observations, and the volcanic activity from which it originated might be of such a low intensity that it was not recognized in distant monitoring systems such as seismic observations.

The small volume of the drifting pumice indicated the possibility of the re-activation of the pumice that had previously washed ashore. The estimated source area included Sumisujima volcanic island (Fig. 4), which might be a potential source region for this re-activation. While our simulation did not exclude this possibility, AIST (2023a) reported that the likelihood of re-activation is low based on the geological observations of the sampled pumice, as discussed later.

4.3 Sampling Floating Pumice

Following the discovery of the pumice near Torishima Island by the observation aircraft, the JMA's oceanographic observation ship "KEIFUMARU," sailed from October 27–31 in the area from 28°N138°E to 30°N140°E to search for the pumice (Japan Meteorological Agency, 2023b). They sampled the pumice scattered on the sea surface southwest of Torishima Island at ca. 100 km from Torishima Island.

White pumice was collected around 12:00 on October 27 (JST) at N29°18′, E140°00′. They mostly have sizes of 1 cm to several centimeters, with the largest being slightly over 10 cm (Japan Meteorological Agency, 2023b). According to AIST (2023a), the preservation of fragile surface structures, predominantly angular shapes, and the almost absence of biological attachments excludes the possibility of them being drifted for a long period of several months or more. For similar reasons, the possibility of them being re-drifted beach-deposited pumice is considered low (AIST, 2023a). Therefore, it is considered that the white pumice had been recently produced by volcanic activity, and AIST (2023a) concluded that it is highly likely to be part of the pumice raft observed from the air by the Japan Coast Guard on October 20 (JST).

In addition to white pumice, "KEIFUMARU" collected another pumice type, gray pumice, on October 27, 28, and 31 (JST), at locations N29°54′,E139°34′, N29°54′,E139°32′, and N29°02′,E138°00′, respectively (Japan Meteorological Agency, 2023b; AIST, 2023a). The sampling location of gray pumice was several tens of kilometers far away from that of the white pumice. Most of this pumice is well-rounded, with the largest being approximately 3 cm, and many others being fine-grained, less than 1 cm, as seen in the published photos. The pumice universally has biological remains attached, particularly many serpulid worm tubes, approximately 1 mm in diameter. Serpulid worms are relatively late colonizers (c.a. 6 months) of floating material (Mesaglio et al., 2021). In addition, the pumice found on October 31 was reported to be scattered with plastic waste (Japan Meteorological Agency, 2023b). These characteristics suggest long-term drifting, indicating that the gray pumice had either drifted for an extended period or underwent repeated re-drifting. AIST (2023b) concluded that this pumice was likely sourced from the 2021 eruption of Fukutoku-Okanoba, based the chemical composition of the basaltic glass and the presence of dark inclusions similar to the drifting pumice reported by Yoshida et al. (2022). Clear differences in the sample location, biological attachment, and geochemistry between the white and gray pumices exclude the possibility of their coexistence within the same pumice raft during their drifting.

4.4 Implications of Marine Organisms Attached to White Pumice

According to the AIST's November 7, 2023, report (AIST, 2023a), the white pumice collected by "KEIFUMARU" around 12:00 on October 27 had almost no attached biological remains, with only three goose barnacles less than 4 mm in length attached. Based on their morphological characteristics, they were identified as *Lepas anserifera*.

Lepas barnacles are rapid colonizers of floating materials (< 17 days), and their growth rate in the capitular-length direction ranges from 0.33 to 1.45 mm/day (MacIntyre, 1966; Inatsuchi et al., 2010; Mesaglio et al., 2021; Watanabe et al., 2024) The size of its cyprid or settlement-stage larvae is approximately 1.3 mm; therefore, it is plausible that Lepas barnacles settled on the pumice formed and released less than approximately 20 days before collection.

Although growth rates vary depending on the environment, based on these experimental growth rates, it is unlikely that *L. anserifera* attached more than half a month before collection on October 27. This is consistent with the fact that the pumice is the same as that observed by the aircraft on October 20.

4.5 Implications of Geochemical Characteristics of White Pumice

According to ERI, U Tokyo (2023) and AIST (2023a), the whole-rock chemical composition obtained via XRF analysis indicated dacitic to rhyolitic compositions with the SiO_2 contents ranging from 70.5 to 74.6 wt.% and the $Na_2O + K_2O$ contents ranging from 6.3 to 6.7 wt.%. These compositions differ from the recent eruptive products of active volcanoes on the volcanic front of the Izu–Ogasawara region (e.g., Nishinoshima, Iwo Jima, and Fukutoku-Okanoba). Additionally, ERI, U Tokyo (2023) and AIST (2023a) suggested that these pumices might be derived from rhyolitic volcanoes distributed along the back-arc rift zone west of the volcanic front (e.g., the Torishima depression). Furthermore, the whole-rock trace element composition (i.e., Ba/La and La/Sm) showed values similar to those of volcanic ejecta from submarine volcanoes in the back-arc rift zone (North and South Sumisu Basins, Hachijo Basin), as reported by AIST (2023b).

Tamura et al. (2009) geochemically identified three types of Quaternary rhyolites in the Izu-Ogasawara arc front, which are closely related in terms of the volcano type and crustal structure. The predominantly basaltic islands in the volcanic front produce small volumes of rhyolites (R1), submarine calderas in the volcanic front erupt mostly rhyolites (R2), and seamounts, knolls, and pillow ridges in the back-arc extensional zone are mostly basaltic but also contain rhyolites (R3). In addition to the possibility that the white pumice corresponded to R3 (ERI, U Tokyo, 2023; AIST, 2023b), we proposed that it might correspond to R2.

The back-tracking drift simulation used in this study demonstrated that the floating pumice drifted southward around the back-arc rift on the west side of the active volcanic front, reaching the observation position on October 20. Additionally, the source analysis suggested that the pumice could have originated from around the back-arc side of the Sumisujima and Myojinsho area, which included the back-arc extensional zone as well as submarine caldera or submarine volcanoes. The simulation results were consistent with geochemical analyses.

4.6 Pumice Tracing to Infer Hidden Submarine Volcanism

While some submarine volcanic eruptions, such as the 2021 Fukutoku-Oka-no-Ba and 2022 Hunga Tonga–Hunga Ha'apai eruptions, were clearly observed by geophysical measurements and confirmed visually, others, such as the 2012 Havre and 2019 Tonga F eruptions, were recognized only after the discovery of pumice rafts and subsequent investigations to identify the eruptions. In addition, deep-sea submarine volcanoes are generally believed to exhibit effusive rather than explosive eruptions (Kano, 2003; Allen et al., 2010; Manga et al., 2018; Cas & Simmons, 2018), making it extremely challenging to detect these volcanic activities. AIST (2023a) reported that the white pumice discovered near Torishima Island notably lacked prominent quench textures, indicating that eruption occurred in deep-sea rather than in shallow waters. While detailed satellite imagery investigations have identified eruptions, such as Havre in 2012 and Tonga F in 2019, it is particularly difficult to detect smaller-scale eruptions from satellite images because they produce less pumice and are presumably smaller in scale. At present (September 2024), there have been no reports of such traces being found by satellite imagery for eruptions related to the pumice found on October 20.

However, such "unknown" eruptions of submarine volcanoes that eject small amounts of pumice might usually go undetected and therefore, might be not as rare as thought. This study represents the first case in which a back-tracking drift simulation has proven effective in pinpointing the eruption sites of such unknown submarine volcanoes. In the future, by using satellite imagery observations and autonomous drones, it might be possible to automatically detect pumice rafts (e.g. Zheng et al., 2022). Combining this with back-tracking simulations, numerous small-scale submarine volcanic activities that were previously invisible could be detected. In addition to locating the eruption site, detailed analyses of the pumice microstructures and in situ marine surveys are expected to contribute to elucidating the eruption mechanisms and monitoring of submarine volcanic activities.

5 Conclusion

Our study conducted back-tracking drift simulations of floating pumice found near Torishima Island in the Izu–Ogasawara Islands on October 20, 2023. By integrating the ocean current data and surface wind data, we traced the pumice's journey, revealing its likely origin as near the back-arc side region west of Myojinsho and Sumisujima Island 3–5 days before its discovery. This timing and location are not consistent with either the increased seismic activity observed in the region since October or the unexplained tsunami-accompanied earthquake on October 9.

These findings suggest that the pumice originated from an unknown volcanic event, possibly distinct from the activities of known active volcanic sites in the area. Preliminary reports (AIST, 2023a, 2023b; ERI, U Tokyo, 2023) suggest that geochemical analyses indicated a composition consistent with volcanoes in the back-arc rift zone, and the lack of extensive biological traces on the pumice implies a relatively recent eruptive source (AIST, 2023a). These results highlight the significance of back-tracking drift simulations in uncovering hidden submarine volcanic activities and their potential impacts.

Furthermore, our research underscores the challenges in detecting and understanding deep-sea volcanic activities, especially those that are effusive and not immediately apparent. By combining drift simulations with geological, petrological, and biological analyses, we can gain a more comprehensive understanding of such phenomena. This approach not only aids in identifying the sources of marine volcanic events but also contributes to the broader field of submarine geology and volcanic hazard assessment.

6 Open Research

The ocean re-analysis dataset is the operational system for monitoring and forecasting coastal and open-ocean states around Japan GPV, provided by the Japan Meteorological Business Support Center (`http://www.jmbsc.or.jp/en/index-e.html`). The maps in Figure 1 were produced using Generic Mapping Tools v5 (Wessel et al., 2013).

Acknowledgments

This work was supported by JST CREST (JPMJCR1761)and JSPS KAKENHI (JP 20H01986; 21H04750; 22H00251; JP24K01139); and the Cooperative Research Program of the Earthquake Research Institute, University of Tokyo (ERI JURP 2021-B-01; 2022-B-06). The authors thank Dr. S. Tanaka for his comments on the geophysical observation of volcanic activities. The authors also thank Prof. S.E. Bryan and Prof. M. Jutzeler for their constructive comments on the early version of the manuscript.

References

AIST. (2023a, November 7). *Characteristics of the drifting pumice collected near torishima in october 2023 (first report) (in Japanese).* Report for Coordinating Committee for Prediction of Volcanic Eruption `https://www.gsj.jp/hazards/volcano/kazan-bukai/yochiren/torishimakinkai_231109_1.pdf`. (Retrieved on November 26, 2023)

AIST. (2023b, November 15). *Characteristics of the drifting pumice collected near torishima in october 2023 (second report) (in Japanese).* Report for Coordinating Committee for Prediction of Volcanic Eruption `https://www.gsj.jp/hazards/volcano/kazan-bukai/yochiren/torishimakinkai_231115_1.pdf`. (Retrieved on November 26, 2023)

Allen, S. R., Fiske, R. S., & Tamura, Y. (2010). Effects of water depth on pumice formation in submarine domes at Sumisu, Izu-Bonin arc, western Pacific. *Geology*, *38*(5), 391–394.

Al-Qattan, N., Herbert, G. S., Spero, H. J., McCarthy, S., McGeady, R., Tao, R., & Power, A.-M. (2023). A stable isotope sclerochronology-based forensic method for reconstructing debris drift paths with application to the MH370 crash. *AGU Advances*, *4*(4), e2023AV000915. doi: https://doi.org/10.1029/2023AV000915

Amante, C., & Eakins, B. W. (2009). ETOPO1 arc-minute global relief model: procedures, data sources and analysis. Retrieved from `https://repository.library.noaa.gov/view/noaa/1163`

Bryan, S. E., Cook, A., Evans, J., Colls, P., Wells, M., Lawrence, M., ... Leslie, R. (2004). Pumice rafting and faunal dispersion during 2001–2002 in the Southwest Pacific: record of a dacitic submarine explosive eruption from Tonga. *Earth and Planetary Science Letters*, *227*(1-2), 135–154.

Bryan, S. E., Cook, A. G., Evans, J. P., Hebden, K., Hurrey, L., Colls, P., ... Firn, J. (2012). Rapid, long-distance dispersal by pumice rafting. *PloS one*, *7*(7), e40583.

Cas, R. A. F., & Simmons, J. M. (2018). Why deep-water eruptions are so different from subaerial eruptions. *Frontiers in Earth Science*, *6*. doi: 10.3389/feart.2018.00198

Chang, Y.-L. K., McIntosh, I. M., Miyama, T., & Miyazawa, Y. (2023). Projection of August 2021 pumice dispersion from the Fukutoku-Oka-no-Ba eruption in the western North Pacific. *Scientific Reports*, *13*(1), 3945.

Chiang, Y., Huang, P.-C., & Yang, Z.-Y. (2024). Assessment of the fukutoku-okanoba pumice rafts dispersion model using the daily collection data from nuclear power plants seawater intake system. *Nuclear Engineering and Design*, *427*, 113448.

Doucet, A., Godsill, S., & Andrieu, C. (2000). On sequential monte carlo sampling methods for bayesian filtering. *Statistics and computing*, *10*, 197–208.

ERI, U Tokyo. (2023, November 9). 【*Analysis Results*】 *Whole-rock Chemical Composition of Drifting Pumice Collected Near Izu Torishima and Sofugan Rocks (in Japanese).* Report for Coordinating Committee for Prediction of Volcanic Eruption `https://www.eri.u-tokyo.ac.jp/eq/20272/`. (Retrieved on November 26, 2023)

Fauria, K. E., Jutzeler, M., Mittal, T., Gupta, A. K., Kelly, L. J., Rausch, J., ... Retailleau, L. (2023). Simultaneous creation of a large vapor plume and pumice raft by the 2021 fukutoku-oka-no-ba shallow submarine eruption. *Earth and Planetary Science Letters*, *609*, 118076.

Fauria, K. E., Manga, M., & Wei, Z. (2017). Trapped bubbles keep pumice afloat and gas diffusion makes pumice sink. *Earth and Planetary Science Letters*, *460*, 50–59.

Fujioka, K. (1989). Arc volcanism and rifting. *Nature*, *342*(1), 18–20.

Fujiwara, T., Imai, K., Obayashi, M., Yoshida, K., Tada, N., Obana, K., ... Kodaira, S. (2024). The sofu seamount present in the source area of the october 2023 earthquake and tsunami in japan. *Geophysical Research Letters*.

Gilks, W. R., Richardson, S., & Spiegelhalter, D. (1995). *Markov chain monte carlo in practice*. CRC press.

Ikegami, F. (2021). Pumice raft dispersion of fukutoku-oka-no-ba 2021 eruption. *Abstract Vol. Annu. Meet. Volcanol. Soc. Jpn. 2021*, A2-02.

Inatsuchi, A., Yamato, S., & Yusa, Y. (2010). Effects of temperature and food availability on growth and reproduction in the neustonic pedunculate barnacle lepas anserifera. *Marine Biology*, *157*, 899–905.

Iskandar, M. R., Park, Y.-G., Kim, K., Jin, H., Seo, S., & Kim, Y. H. (2023). Tracking the pumice rafts from the Fukutoku-Okanoba submarine volcano with satellites and a Lagrangian particles trajectory model. *Marine Pollution Bulletin*, *193*, 115254. doi: https://doi.org/10.1016/j.marpolbul.2023.115254

Ismail-Zadeh, A., Schubert, G., Tsepelev, I., & Korotkii, A. (2004). Inverse problem of thermal convection: numerical approach and application to mantle plume restoration. *Physics of the Earth and Planetary Interiors*, *145*(1-4), 99–114.

Ito, M., Kuwatani, T., Oyanagi, R., & Omori, T. (2021). Data-driven analysis of nonlinear heterogeneous reactions through sparse modeling and bayesian statistical approaches. *Entropy*, *23*(7), 824.

JAMSTEC. (2023a, October 30). *About the Seismic Activity Near Torishima in October 2023 and the Tsunami that was Disproportionately Large Compared to the Earthquake Magnitude (in Japanese).* Column by researchers `https://www.jamstec.go.jp/j/pr/topics/column-20231030/`. (Retrieved on November 26, 2023)

JAMSTEC. (2023b, October 24). *Future Drift of the Floating Pumice Observed Near Torishima (Preliminary Rapid Report) (in Japanese).* Report for Coordinating Committee for Prediction of Volcanic Eruption `https://www.jamstec.go.jp/rimg/j/topics/20231026/`. (Retrieved on November 26, 2023)

JAMSTEC. (2023c, November 8). *Regarding an Emergency Survey Voyage in the Waters near Torishima by the Oceanographic Research Ship 'Kaimei' (in Japanese).* Press Release `https://www.jamstec.go.jp/j/about/press_release/20231108/`. Retrieved 2023-11-26, from `https://www.jamstec.go.jp/j/about/press_release/20231108/` (Retrieved on November 26, 2023)

JAMSTEC. (2023d, November 21). *Regarding an Emergency Survey Voyage in the Waters near Torishima by the Oceanographic Research Ship 'Kaimei' (Preliminary report) (in Japanese).* Press Release `https://www.jamstec.go.jp/j/about/press_release/20231121/`. (Retrieved on November 26, 2023)

Jansen, E., Coppini, G., & Pinardi, N. (2016). Drift simulation of MH370 debris using superensemble techniques. *Natural Hazards and Earth System Sciences*, *16*(7), 1623–1628. doi: 10.5194/nhess-16-1623-2016

Japan Coast Guard. (2023a). *Kuroshio current axis. [Data]* [dataset]. Retrieved from `http://www.mirc.jha.jp/products/KCP/`

Japan Coast Guard. (2023b, October 20). *Regarding the floating objects near Torishima observed on October 20th (in Japanese).* `https://www.kaiho.mlit.go.jp/info/kouhou/post-1041.html`. (Retrieved on November 26, 2023)

Japan Meteorological Agency. (2013a). Meso-Scale Model (JMA-MSM1206). Outline of the operational numerical weather prediction at the Japan Meteorological Agency. *JMA*, 71–93. Retrieved from `http://www.jma.go.jp/jma/jma-eng/jma-center/nwp/outline2019-nwp/index.htm`

Japan Meteorological Agency. (2013b). National Catalogue of the Active Volcanoes in Japan, 4th Edition. Retrieved from `https://www.data.jma.go.jp/svd/vois/data/tokyo/STOCK/souran_eng/menu.htm`

Japan Meteorological Agency. (2023a, October 9). *Report on Earthquake near Torishima Island around 5:25 on October 9, 2023 (2nd report) (in Japanese).* `https://www.jma.go.jp/jma/press/2310/09b/202310091100.html`. (Retrieved October 19, 2023)

Japan Meteorological Agency. (2023b, November 1). *Sampling of Pumice in the Waters Near Torishima by the Marine Meteorological Observation Ship 'Keifu-Maru (in Japanese).* Press Release Materials for Fiscal Year 2023 `https://www.jma.go.jp/jma/press/2311/01b/20231101_keihu-karuishi.html`. (Retrieved on November 26, 2023)

Japan Meteorological Agency. (2024). Meso-scale model (MSM) grid data, Information catalog of Japan Meteorological Agency. Retrieved from `https://www.data.jma.go.jp/suishin/cgi-bin/catalogue/make_product_page.cgi?id=MesModel`

Jutzeler, M., Marsh, R., Carey, R. J., White, J. D., Talling, P. J., & Karlstrom, L. (2014). On the fate of pumice rafts formed during the 2012 Havre submarine eruption. *Nature communications*, *5*(1), 3660.

Jutzeler, M., Marsh, R., van Sebille, E., Mittal, T., Carey, R. J., Fauria, K. E., … McPhie, J. (2020). Ongoing dispersal of the 7 August 2019 pumice raft from the Tonga arc in the southwestern Pacific Ocean. *Geophysical Research Letters*, *47*(5), e1701121.

Kano, K. (2003). Subaqueous pumice eruptions and their products: A review. *Washington DC American Geophysical Union Geophysical Monograph Series*, *140*, 213–229.

Kitagawa, G. (1987). Non-gaussian state—space modeling of nonstationary time series. *Journal of the American statistical association*, *82*(400), 1032–1041.

Knafelc, J., Bryan, S. E., Jones, M. W., Gust, D., Mallmann, G., Cathey, H. E., … Howard, D. L. (2022). Havre 2012 pink pumice is evidence of a short-lived, deep-sea, magnetite nanolite-driven explosive eruption. *Communications Earth & Environment*, *3*(1), 19.

Kubota, T., Sandanbata, O., Saito, T., & Matsuzawa, T. (2024). Accelerating seafloor uplift of submarine caldera near sofugan volcano, japan, resolved by distant tsunami recordings. *Geophysical Research Letters*, *51*(12), e2024GL108415.

Kuroda, H. (2023). History, current status, and future vision of particle-tracking simulation applied to marine biology, fisheries science, and ecological engineering around japan. *Fisheries Science*, *89*(2), 129–146.

Kuwatani, T., Kitao, K., Nishikawa, H., Tada, N., & Watanabe, H. K. (2023). Visualization of simulated paths of drifting pumices using point cloud PNG:towards the construction of hazard assessment system for drifting pumices (in Japanese with English Abstract). *Geoinformatics*, *34*(3), 61-68. doi: 10.6010/geoinformatics.34.3_61

Kuwatani, T., Nagao, H., Ito, S.-i., Okamoto, A., Yoshida, K., & Okudaira, T. (2018). Recovering the past history of natural recording media by bayesian inversion. *Physical Review E*, *98*(4), 043311.

Kuwatani, T., Nagata, K., Okada, M., & Toriumi, M. (2012). Precise estimation of pressure–temperature paths from zoned minerals using markov random field modeling: theory and synthetic inversion. *Contributions to Mineralogy and Petrology*, *163*, 547–562.

MacIntyre, R. (1966). Rapid growth in stalked barnacles. *Nature*, *212*(5062), 637–638.

Maeno, F., Kaneko, T., Ichihara, M., Suzuki, Y. J., Yasuda, A., Nishida, K., & Ohminato, T. (2022). Seawater-magma interactions sustained the high column during the 2021 phreatomagmatic eruption of Fukutoku-Oka-no-Ba. *Communications Earth & Environment*, *3*(1), 260.

Manga, M., Fauria, K. E., Lin, C., Mitchell, S. J., Jones, M. P., Conway, C. E., … Tani, K. (2018). The pumice raft-forming 2012 Havre submarine eruption was effusive. *Earth and Planetary Science Letters*, *489*, 49-58. doi: https://doi.org/10.1016/j.epsl.2018.02.025

Matsumura, T., Kuwayama, Y., Ueki, K., Kuwatani, T., Ando, Y., Nagata, K., … Nagao, H. (2021). Bayesian modeling of the equation of state for liquid iron in earth's outer core. *Journal of Geophysical Research: Solid Earth*, *126*(12), e2021JB023062.

Mesaglio, T. P., Schilling, H. T., Adler, L., Ahyong, S. T., Maslen, B., & Suthers, I. M. (2021). The ecology of lepas-based biofouling communities on moored and drifting objects, with applications for marine forensic science. *Marine Biology*, *168*, 1–16.

Metropolis, N., Rosenbluth, A. W., Rosenbluth, M. N., Teller, A. H., & Teller, E. (1953). Equation of state calculations by fast computing machines. *The journal of chemical physics*, *21*(6), 1087–1092.

Mitchell, S. J., Fauria, K. E., Houghton, B. F., & Carey, R. J. (2021). Sink or float: microtextural controls on the fate of pumice deposition during the 2012 submarine Havre eruption. *Bulletin of Volcanology*, *83*, 1–20.

Miyama, T. (2023). Simulation of drifting pumice from the fukutoku-oka-no-ba submarine volcano (in Japanese). *Journal of the Japan Society for Marine Surveys and Technology*, *35*(1), 19–21.

Mizutani, A., & Melgar, D. (2023). Potential volcanic origin of the 2023 short-period tsunami in the izu islands, japan. *Seismica*, *2*(2).

Morishige, M., & Kuwatani, T. (2020). Bayesian inversion of surface heat flow in subduction zones: a framework to refine geodynamic models based on observational constraints. *Geophysical Journal International*, *222*(1), 103–109.

Nakao, A., Kuwatani, T., Ito, S.-i., & Nagao, H. (2024a). Adjoint-based data assimilation for reconstruction of thermal convection in a highly viscous fluid from surface velocity and temperature snapshots. *Geophysical Journal International*, *236*(1), 379–394.

Nakao, A., Kuwatani, T., Ito, S.-i., & Nagao, H. (2024b). Adjoint-based marker-in-cell data assimilation for constraining thermal and flow processes from lagrangian particle records. *Authorea Preprints*.

Nishikawa, H., Kuwatani, T., Tada, N., & Kayama Watanabe, H. (2023). Simulated distributions of pumice rafts in Japan following eruptions at volcanic islands and submarine volcanoes. *Progress in Earth and Planetary Science*, *10*(1), 1–20.

Okubo, A. (1971). Oceanic diffusion diagrams. In *Deep sea research and oceanographic abstracts* (Vol. 18, pp. 789–802).

Omori, T., Kuwatani, T., Okamoto, A., & Hukushima, K. (2016). Bayesian inversion analysis of nonlinear dynamics in surface heterogeneous reactions. *Physical Review E*, *94*(3), 033305.

Putman, N. F., Goni, G. J., Gramer, L. J., Hu, C., Johns, E. M., Trinanes, J., & Wang, M. (2018). Simulating transport pathways of pelagic sargassum from the equatorial atlantic into the caribbean sea. *Progress in oceanography*, *165*, 205–214.

Sandanbata, O., Satake, K., Takemura, S., Watada, S., Maeda, T., & Kubota, T. (2024). Enigmatic tsunami waves amplified by repetitive source events near sofugan volcano, japan. *Geophysical Research Letters*, *51*(2), e2023GL106949.

Sandanbata, O., Watada, S., Satake, K., Kanamori, H., Rivera, L., & Zhan, Z. (2022). Sub-decadal volcanic tsunamis due to submarine trapdoor faulting at sumisu caldera in the izu–bonin arc. *Journal of Geophysical Research: Solid Earth*, *127*(9), e2022JB024213. doi: https://doi.org/10.1029/2022JB024213

Tada, N., Nishikawa, H., Ichihara, H., Watanabe, H. K., & Kuwatani, T. (2021). Drift of an ocean bottom electromagnetometer from the Bonin to Ryukyu Islands: estimation of the path and travel time by numerical tracking experiments. *Earth, Planets and Space*, *73*(1), 224.

Tamura, Y., Gill, J. B., Tollstrup, D., Kawabata, H., Shukuno, H., Chang, Q., … others (2009). Silicic magmas in the izu–bonin oceanic arc and implications for crustal evolution. *Journal of Petrology*, *50*(4), 685–723.

Trinanes, J. A., Olascoaga, M. J., Goni, G. J., Maximenko, N. A., Griffin, D. A., & Hafner, J. (2016). Analysis of flight MH370 potential debris trajectories using ocean observations and numerical model results. *Journal of Operational Oceanography*, *9*(2), 126–138.

Van Sebille, E., Griffies, S. M., Abernathey, R., Adams, T. P., Berloff, P., Biastoch, A., … others (2018). Lagrangian ocean analysis: Fundamentals and practices. *Ocean modelling*, *121*, 49–75.

Watanabe, K. H., Nagai, Y., Sakai, S., Kobayashi, G., Yamamori, L., Tada, N., … Yusa, Y. (2024). Heterogeneous shell growth of a neustonic goose barnacle *Lepas anserifera*. *Marine Biology*, *171*(1), 161. doi: https://doi.org/10.1007/s00227-024-04481-8

Wessel, P., Smith, W. H., Scharroo, R., Luis, J., & Wobbe, F. (2013). Generic mapping tools: improved version released. *Eos, Transactions American Geophysical Union*, *94*(45), 409–410.

Yoshida, K., Tamura, Y., Sato, T., Hanyu, T., Usui, Y., Chang, Q., & Ono, S. (2022). Variety of the drift pumice clasts from the 2021 Fukutoku-Oka-no-Ba eruption, Japan. *Island Arc*, *31*(1), e12441.

Yuasa, M. (1995). Myojin knoll, Izu-Ogasawara arc : Submersible study of submarine pumice volcano. *Bulletin of the Volcanological Society of Japan*, *40*(4), 277-284. doi: 10.18940/kazan.40.4_277

Zheng, M., Mittal, T., Fauria, K. E., Subramaniam, A., & Jutzeler, M. (2022). Pumice raft detection using machine-learning on multispectral satellite imagery. *Frontiers in Earth Science*, *10*, 838532.

Supporting Information for "Estimating the Source of Floating Pumice Found near Torishima Island, Japan: A Back-Tracking Drift Simulation Approach "

T. Kuwatani[1], H. Nishikawa[2], Y. Tanaka[2,3], H. K. Watanabe[4], N. Tada[1], A. Nakao[5,1], Y. Tamura[1], and S. Ono[1]

[1]Volcanoes and Earth's Interior Research Center (VERC), Research Institute for Marine Geodynamics (IMG), Japan Agency for Marine-Earth Science and Technology (JAMSTEC), 2-15 Natsushima-cho, Yokosuka, Kanagawa237-0061, Japan .

[2]Research Institute for Value-Added-Information Generation(VAiG), Japan Agency for Marine-Earth Science and Technology, 3173-25 Showa-machi, Kanazawa-ku, Yokohama, Kanagawa 236-0001, Japan

[3]Ocean Eyes Co., Ltd., Uradeyamacho 308, Nakagyo-ku, Kyoto-shi, Kyoto 604-8155, Japan

[4]Institute for Extra-Cutting-Edge Science and Technology Avant-Garde Research (X-Star), Japan Agency for Marine-Earth Science and Technology, 2-15 Natsushima-cho, Yokosuka, Kanagawa237-0061, Japan

[5]Graduate School of Engineering Science, Akita University, Akita 010-8502, Japan

Contents of this file

Additional Supporting Information (Files uploaded separately)

1. Captions for Movies S1 to S8

Introduction

This supporting information includes description of movie files for the results of the back-tracking simulation.

Movie S1. Without windage in the forward time direction

Movie S2. Without windage in the backward time direction

Movie S3. With 1% windage in the forward time direction

Movie S4. With 1% windage in the backward time direction

Movie S5. With 3% windage in the forward time direction

Movie S6. With 3% windage in the backward time direction

Movie S7. With 5% windage in the forward time direction

Movie S8. With 5% windage in the backward time direction